Global and Planetary Change 124 (2015) 79–94

Contents lists available at ScienceDirect

Global and Planetary Change

journal homepage: www.elsevier.com/locate/gloplacha

Trends and variability of daily temperature extremes during 1960–2012 in the Yangtze River Basin, China

Yinghui Guan [a,b], Xunchang Zhang [c], Fenli Zheng [a,b,*], Bin Wang [d]

[a] College of Resources and Environment, State Key Laboratory of Soil Erosion and Dryland Farming on the Loess Plateau, Northwest A&F University, No.3 Taicheng Rd.,Yangling, 712100 Shaanxi, P. R. China
[b] Institute of Soil and Water Conservation, CAS & MWR, No.26 Xinong Rd., Yangling, 712100 Shaanxi, P. R. China
[c] USDA-ARS Grazinglands Research Laboratory, 7207 W. Cheyenne St., El Reno, OK 73036, USA
[d] College of Soil and Water Conservation, Beijing Forestry University, No.35 Tsinghua east Rd., Beijing, 100083, P. R. China

ARTICLE INFO

Article history:
Received 22 June 2014
Received in revised form 14 November 2014
Accepted 19 November 2014
Available online 26 November 2014

Keywords:
Yangtze River Basin
Temperature extremes
Trends
Climate variability
Climate indices

ABSTRACT

The variability of surface air temperature extremes has been the focus of attention during the past several decades, and may exert a great influence on the global hydrologic cycle and energy balance through thermal forcing. Based on daily minimum (TN) and maximum temperature (TX) observed by the China Meteorological Administration at 143 meteorological stations in the Yangtze River Basin (YRB), a suite of temperature indices recommended by the Expert Team on Climate Change Detection and Indices, with a primary focus on extreme events, were computed and analyzed for the period of 1960–2012 for this area. The results show widespread significant changes in all temperature indices associated with warming in the YRB during 1960–2012. On the whole, cold-related indices, i.e., cold nights, cold days, frost days, icing days and cold spell duration index significantly decreased by −3.45, −1.03, −3.04, −0.42 and −1.6 days/decade, respectively. In contrast, warm-related indices such as warm nights, warm days, summer days, tropical nights and warm spell duration index significantly increased by 2.95, 1.71, 2.16, 1.05 and 0.73 days/decade. Minimum TN, maximum TN, minimum TX and maximum TX increased significantly by 0.42, 0.18, 0.19 and 0.14 °C/decade. Because of a faster increase in minimum temperature than maximum temperature, the diurnal temperature range (DTR) exhibited a significant decreasing trend of −0.09 °C/decade for the whole YRB during 1960–2012. However, the decreasing trends all occurred in 1960–1985, while increasing trends though insignificant were found in all sub-regions and the whole YRB during 1986–2012. Geographically, stations in the eastern Tibet Plateau and northeastern YRB showed stronger trends in almost all temperature indices. Time series analysis indicated that the YRB was dominated by a general cooling trend before the mid-1980s, but a warming trend afterwards. In general, the overall warming in the YRB was mainly due to the warming in 1986–2012. Strong relationships between temperature trends and elevation were detected in this study. The warming rates increased with elevation when elevation is above 350 m, but decreased with elevation when elevation is below 350 m.

1. Introduction

There is a general consensus within the climate community that any change in the frequency or intensity of extreme climate events would have more serious and profound impacts on agriculture, ecosystems and human society through various ways (e.g., floods, droughts, hurricanes, storms, extreme heat and cold, etc.) than changes in the mean values (Katz and Brown, 1992; Kunkel et al., 1999; Easterling et al., 2000a, 2000b; Meehl et al., 2000; New et al., 2006; IPCC, 2007; Su et al., 2008; Xu et al., 2009; You et al., 2011; Li et al., 2012b; Fu et al., 2013). Some types of extreme events are expected to continue and occur more frequently due to increased emissions of anthropogenic greenhouse gas in the future (Hegerl et al., 2004; Vincent et al., 2005; IPCC, 2007; Trenberth et al., 2007). As a result, characterizing possible changes and variability in climatic extremes has been strongly advocated (Moberg et al., 2006; Vincent and Mekis, 2006) and is usually the hot topic for government, public and the climatic research community in particular (Su et al., 2008; Zhang et al., 2008; Xu et al., 2009). Climate variability is largely influenced by temperature change, which is particularly important through its role in the global climate system and energy cycles. Meteorologists and hydrologists have indicated that increasing

Abbreviations: ETCCDI, Expert Team on Climate Change Detection and Indices; TN10P, cold nights; TN90P, warm nights; TX10P, cold days; TX90P, warm days; FD, frost days; SU, summer days; ID, icing days; TR, tropical nights; TNn, minimum TN; TNx, maximum TN; TXn, minimum TX; TXx, maximum TX; CSDI, cold spell duration index; WSDI, warm spell duration index; DTR, diurnal temperature range; TN, daily minimum temperature; TX, daily maximum temperature; CV, coefficient of variance

* Corresponding author at: 26 Xinong Rd., Yangling, 712100 Shaanxi, P. R. China. Tel.: +86 29 87013205; fax: +86 29 87012210.
E-mail addresses: gyhdem@aliyun.com (Y. Guan), flzh@ms.iswc.ac.cn (F. Zheng).

http://dx.doi.org/10.1016/j.gloplacha.2014.11.008
0921-8181/

temperatures can speed up and intensify the climatic and hydrological cycles that, in turn, possibly result in changes in global precipitation amounts and intensity, river flow regimes, soil moisture and evapotranspiration rates (Loáiciga et al., 1996; Kunkel et al., 1999; Labat et al., 2004; Zhai et al., 2005). It is also well documented in several studies how the extreme cold or hot temperature events can increase human mortality and morbidity (Kunkel et al., 1999; Huynen et al., 2001; Ma et al., 2011). However, the variability of climatic extremes in different climate regions tends to be different on account of the huge differences in climatic background, climate driving forces and regional characteristics (Li et al., 2011a). In this context, there is a great demand for quantifying climate changes and variability in temperature extremes at a regional or local scale.

The Yangtze River is the longest river in China and the third longest in the world. The importance of the Yangtze River lies not only in its geographical position, sheer size and complex geomorphology, but also in the way that the river plays an important role in the regional water cycle, energy balance, climate change and ecosystems as well as in China's economic and social development (Zhang et al., 2008; Sang et al., 2012). However, climate conditions in the Yangtze River Basin (YRB) greatly changed along with population increase, rapid urbanization, land use/land cover change and dramatic economic development over the past several decades (Sang et al., 2012). This further intensified the extreme temperature events in YRB, which exerted great influence on human health and wellbeing (Tan et al., 2007; Gao, 2009; Li et al., 2011a). For example, the heat waves in both 1998 and 2003 led to elevated mortality in Shanghai (Tan et al., 2007). The unprecedented ice freezing and snow disasters in south China during 2008 killed 107 people, which was the worst in the past 50 years and the minimum temperatures broke the 57-year records (Gao, 2009). In summer 2013, the strongest hot spells since 1951 seriously impacted the south China. Persistent heat wave and lack of rain resulted in severe droughts, causing a direct economic loss of more than 8 billion US$ (The China Meteorological Administration, 2013). Luber and McGeehin (2008) suggested that extreme heat waves are the most prominent cause of human mortality associated with weather in America, and responsible for more deaths annually than floods, hurricanes, earthquakes and tornadoes combined. Besides, high temperatures can cause outbreaks of infectious diseases, respiratory illnesses, tuberculosis, and even worsen ‘lifestyle’ diseases such as hypertension and diabetes (Harlan and Ruddell, 2011). Furthermore, the increasing temperatures affect soil erosion indirectly in several ways (O'Neal et al., 2005), and can change heat and water conditions as well as other environment factors in some regions, vary the length of potential growing season, affect cropping systems and plant growth (Zhang et al., 2013). Nowadays, the YRB is becoming increasingly sensitive and vulnerable to climate change, particularly to the severe and extreme weather (Su et al., 2006; Jiang et al., 2007; Zhang et al., 2008; Xu et al., 2009; Sang et al., 2012). As the basin is densely populated and highly industrialized, the effects tend to be more devastating (Jiang et al., 2007). Against this background, research on trends and variability of temperature extremes in YRB is therefore becoming an imperative task.

According to previous studies, significant increasing trends were detected in 1-day minimum temperature in summer and winter over the YRB, but there was no significant trend for 1-day maximum temperature (Su et al., 2006). Zhang et al. (2005a) explored the monthly mean temperature trends of 51 stations in the YRB from 1950–2012, and concluded that the middle and lower YRB was dominated by somewhat downward temperature trend while upward temperature trend occurred in the upper YRB. Liang et al. (2008) reconstructed the mean summer minimum temperature for the Tibet region of the YRB. This reconstruction successfully captured recent abrupt changes in climate and agreed well with other temperature reconstructions for the Tibetan Plateau. Recently, the spatial and temporal variability of daily minimum, mean and maximum temperature in the YRB were studied by Sang et al. (2012). Results indicated that more complex temperature variability in the middle YRB was detected in terms of the rugged topography, and mean temperatures had more complex variability than minimum and maximum temperatures. Meanwhile, diurnal temperature range (DTR) showed both negative and positive magnitudes in different decades during 1961–2010. In addition, Wang et al. (2013b) found that mean annual temperature over Sichuan province (the upper YRB) increased at a rate of 0.17 °C/decade during 1960–2009, and a significant upward trend of 0.26 °C/decade was detected for winter. The mean annual temperature in the eastern and central Tibet Plateau also increased significantly since the 1960s, especially after the 1980s, and the warming in winter and autumn (0.40 and 0.26 °C/decade respectively) contributed most to the annual trend of 0.25 °C/decade (You et al., 2010b). The temperature of the warmest and coldest nights and the number of extreme warm days and nights increased significantly in southwestern China during 1961–2008, while the number of frost days and DTR decreased significantly, but the decreasing trend of icing days was insignificant (Li et al., 2012b). To date, the most extensive research on changes in temperature extremes in YRB was conducted by Wang et al. (2014). But in general, the trends and variability in temperature extremes have not been investigated systematically and deeply in the YRB. One shortcoming comes from that most previous studies focused on either mean temperature changes (Zhang et al., 2005a; Liang et al., 2008; You et al., 2010b; Sang et al., 2012; Wang et al., 2013b), or only parts of YRB (You et al., 2008; Li et al., 2012b; Wang et al., 2013b, 2013c), or quantifying the trends and variability using only a few simple extreme climate indices (Su et al., 2006; Xu et al., 2009; Li et al., 2012b). Another shortcoming is the use of inappropriate trend computation methods. Some studies (Su et al., 2006; You et al., 2008; Wang et al., 2013b, 2014) used the ordinary least squares to detect trends, but this method is sensitive to outliers or extremes that often occur in extreme events (Vincent et al., 2005; Vincent and Mekis, 2006).

To overcome the above shortcomings, the main objectives of this study are (1) to analyze the trends in statistical parameters of daily minimum and maximum temperature for the entire YRB; (2) to investigate the spatial distribution of temperature extremes in YRB during 1960–2012 based on 15 climate indices proposed by the Expert Team on Climate Change Detection and Indices; (3) to explore the temporal changes of extreme temperature indices during 1960–2012 and two sub-periods 1960–1985 and 1986–2012. We intended to (1) provide a better understanding of climate changes and variability in frequency, amplitude and persistence of temperature extremes in both time and space in the entire YRB during 1960–2012; (2) offer the most comprehensive and detailed information on trends and variability of temperature extremes that can help government policy makers and urban planners to establish and improve risk management systems to effectively mitigate the adverse impacts of climate extremes.

2. Study area

The Yangtze River (Fig. 1), situated between latitudes 25°N–35°N and longitudes 91°E–122°E, is about 6300 km long and has a drainage area of 1.80 million km^2, which accounts for nearly 20% of the landmass of China (Li et al., 2011a). The river originates from the Qinghai-Tibet Plateau that has long been known as the roof of the world, and flows across three distinct terrains from the headwater region to the East China Sea at Shanghai city, with a 6000 m elevation drop (Zhao et al., 2009). In general, the upper reaches of the Yangtze River, from its source area to Yichang, is predominantly mountainous terrain. The middle reaches, from Yichang to Hukou, is mainly fluvial plains. However, the lower reaches, from Hukou to the estuary, is extremely flat and only 4–10 m above the mean sea level (Yu et al., 2009). Apart from some areas located in the Tibet Plateau, the YRB, for the most part, is affected by a subtropical monsoon climate (Zhao et al., 2009). Three types of monsoon prevail in the YRB. In winter, the whole YRB is under the control of the Siberian northwest monsoon. In summer, the East Asia

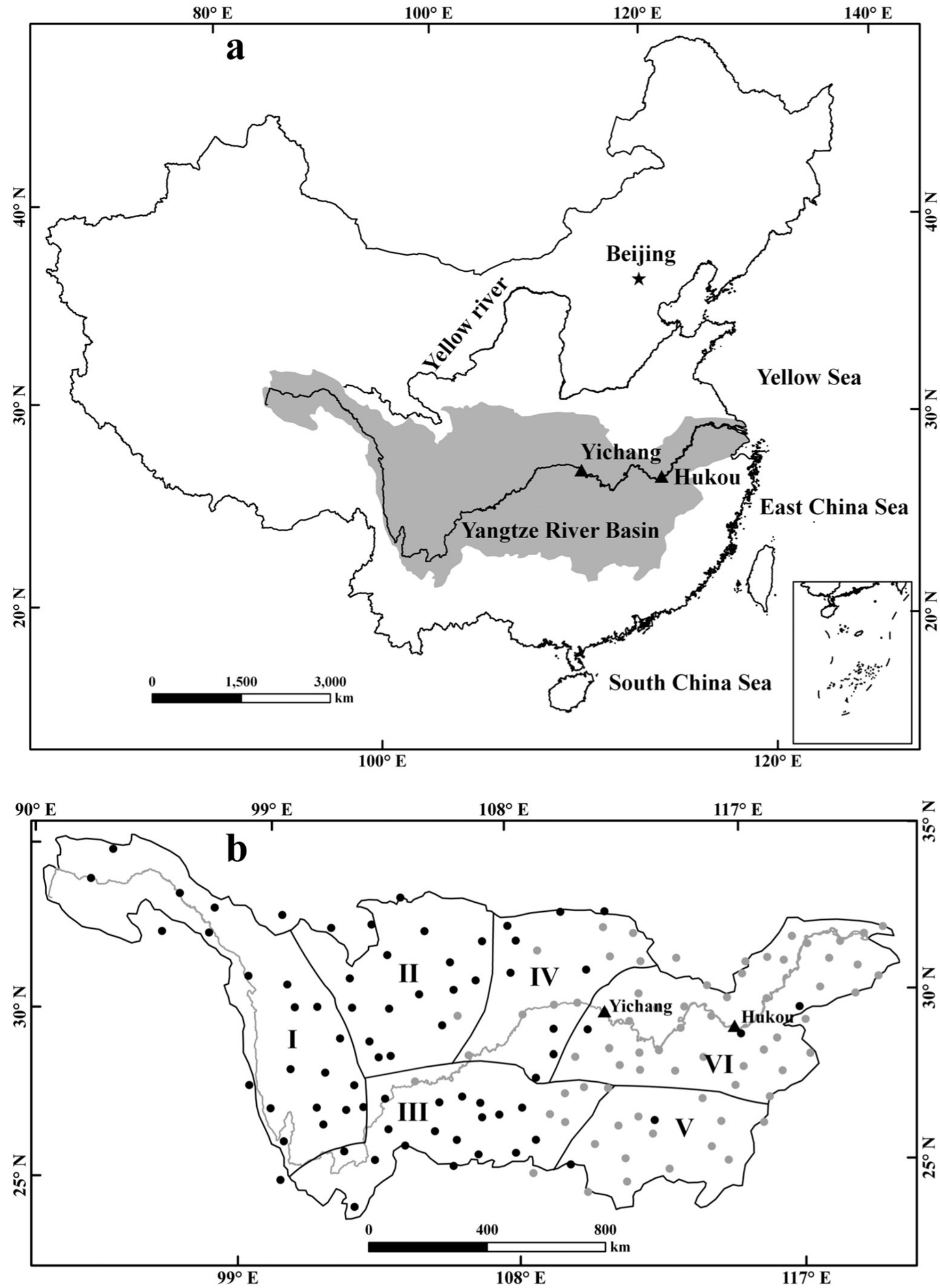

Fig. 1. The location of the Yangtze River Basin in China (a) and the location of 143 meteorological stations and six regions, including the eastern Tibet plateau (I), the mid-western (II), the south-central (III), the mid-eastern (IV), the southeastern (V), and the northeastern (VI) in the Yangtze River Basin(b). Meteorological stations with elevation >350 m is set to black and stations with elevation ≤350 m is gray.

monsoon predominantly influences the middle and lower reaches, i.e., regions V and VI, while the Indian southwest monsoon mainly influences the upper reaches, i.e., regions I, II, III and IV (Su et al., 2006; Zhang et al., 2007; Zhao et al., 2009, 2012). The Indian and the East Asian monsoon systems are independent of each other and, at the same time, interact with each other (Ding and Chan, 2005; Zhang et al., 2007). Climatically, the southern part of the basin is adjacent to the tropical zone and the northern part is close to the temperate zone. The annual mean temperature is about 19 and 15 °C respectively in the southern and northern parts in the middle and lower reaches of YRB, but varies a lot in the upper reaches from 17 °C in the Sichuan Basin to no more than 0 °C on the eastern Tibet Plateau (Zhang et al., 2005a). The rugged topography and strong influence of monsoon resulted in distinct climate characteristics and different response sensitivities to global warming in YRB.

Nowadays the YRB is home to more than 440 million people, over 33% of China's population, but the distribution is uneven (Sang et al., 2012). The most sparsely populated region is the highland area in the upper reaches of YRB, while the most densely populated region is the Yangtze River Delta, such as Shanghai where the population density is more than 4600 persons per km^2 (Sang et al., 2012). The three inland cities of Chongqing, Wuhan, Nanjing and the coastal city of Shanghai are among the most important industrial centers of China, and the Yangtze River Delta is among China's most economically developed areas (Sang et al., 2012). These cities contribute considerably to the greenhouse gas emission and make the climate warming more deadly and costly (Zhao et al., 2012).

3. Data and methodology

3.1. Dataset

The time series of daily minimum and maximum temperature measured at 176 meteorological stations were used in this study, which was provided by the China Meteorological Administration (CMA) (http://cdc.cma.gov.cn). The climate data are maintained according to the World Meteorological Organization's (WMO) standards and CMA's Technical Regulation on Weather Observations (Xu et al., 2006). This dataset has gone through the strict quality control procedures (e.g., extreme value test and time consistency test), and has also been widely used in studying climate changes in China (Zhai and Pan, 2003; You et al., 2008; Li et al., 2010, 2012a, 2012b; Wang et al., 2013a, 2013b, 2013c). All of them have the same measured records from 1960–2012 because data before 1960 contains many missing values and gaps. If one station has more than 1% missing data and the missing data in one station exceed three consecutive months, this station was excluded from this study. Finally, 143 available stations scattered in YRB during 1960–2012 were selected for this study. In addition, the YRB is characterized by complex climate systems. To better understand the regional features of these extreme events, the whole YRB was divided into six sub-regions according to the Rotated Empirical Orthogonal Function (REOF) analysis conducted by Su et al. (2008), and then revised in terms of the Mann-Kendall statistic values of 143 stations for 15 temperature indices. The distribution of 143 meteorological stations and six sub-regions over the YRB are depicted in Fig. 1.

3.2. Definition of extreme indices

The Expert Team on Climate Change Detection and Indices (ETCCDI) has been coordinating an international effort to develop, calculate and analyze a suite of 11 precipitation and 16 temperature indices adopted by the Fourth Assessment Report of IPCC (AR4). Different researchers from different regions or countries can calculate the indices exactly the same way such that the results are comparable with analysis conducted elsewhere in the world and can fit seamlessly into the global picture (Karl et al., 1999; Easterling et al., 2003). Therefore, this suite of indices has been widely used to examine changes in extremes in many parts of the world during the last several years (Zhang et al., 2005b; Alexander et al., 2006; Klein Tank et al., 2006; Vincent and Mekis, 2006; You et al., 2008; Rahimzadeh et al, 2009; Li et al., 2012a, 2012b; Wang et al., 2013a, 2013c). Indices irrelevant to the study were omitted, leading to a final selection of 15 temperature indices (Table 1). These indices were chosen to reflect different aspects in climate extremes, e.g., frequency, intensity and duration. It can be divided into five different categories (Alexander et al., 2006): percentile indices including cold nights (TN10P), warm nights (TN90P), cold days (TX10P) and warm days (TX90P); threshold indices including frost days (FD), summer days (SU), icing days (ID) and tropical nights (TR); absolute indices including Minimum TN (TNn), Maximum TN (TNx), Minimum TX (TXn) and Maximum TX (TXx); duration indices including cold spell duration index (CSDI) and warm spell duration index (WSDI) and range indices including diurnal temperature range (DTR). These indices were calculated on an annual basis. It should be noted that all the indices were discussed in Section 4, but some figures were not presented due to their similar changing patterns with those already shown.

3.3. Mann-Kendall test

The Mann-Kendall test (Mann, 1945; Kendall, 1962) based on Sen's slope estimator (Sen, 1968) is a non-parametric test, which is suitable for data that do not follow a normal distribution and less sensitive to outliers (Zhang et al., 2000; Jaagus, 2006; Vincent and Mekis, 2006; Tabari et al., 2011). Moreover, it is simple, robust and can cope with missing values (Kampata et al., 2008; Tabari et al., 2011; Some'e et al., 2012). This method has been widely used to detect trends in meteorological and hydrological time series (Zhang et al., 2000; Cannarozzo et al., 2006; Su et al., 2008; Li et al., 2010; Tabari and Talaee, 2011; Some'e et al., 2012; Wang et al., 2013a, 2013b, 2013c). The test has two important parameters: the statistic Z value that indicates the direction of the trend and the slope magnitude (change per unit time). A detailed description of the trend computation can be found in Tabari and Talaee (2011). In this research, the significance level of $\alpha = 0.05$ was applied.

Considering the rapid warming mainly occurred after the 1980s in YRB (Sang et al., 2012), the whole period was divided into two periods of 1960–1985 and 1986–2012 in this study. The Mann-Kendall test was therefore computed at individual stations for three time periods: 1960–1986, 1986–2012 and 1960–2012. Besides, the test was performed for regionally averaged series of each of the 15 indices. For each index, the time series were calculated by averaging the stations in each sub-region as:

$$x_{r,t} = \frac{1}{n_r}\sum_{i=1}^{n_r} x_{i,t} \tag{1}$$

Table 1
Definitions of 15 temperature indices used in this study.

Index	Description name	Definitions	Units
TN10P	Cold nights	Annual count of days when TN [a] < 10th percentile	days
TN90P	Warm nights	Annual count of days when TN [b] > 90th percentile	days
TX10P	Cold days	Annual count of days when TX < 10th percentile	days
TX90P	Warm days	Annual count of days when TX > 90th percentile	days
FD	Frost days	Annual count of days where TN < 0 °C	days
SU	Summer days	Annual count of days where TX > 25 °C	days
ID	Icing days	Annual count of days where TX < 0 °C	days
TR	Tropical nights	Annual count of days where TN > 25 °C	days
TNn	Minimum TN	Annual minimum value of TN	°C
TNx	Maximum TN	Annual maximum value of TN	°C
TXn	Minimum TX	Annual minimum value of TX	°C
TXx	Maximum TX	Annual maximum value of TX	°C
WSDI	Warm spell duration index	Annual count of days with at least 6 consecutive days when TX > 90th percentile	days
CSDI	Cold spell duration index	Annual count of days with at least 6 consecutive days when TN < 10th percentile	days
DTR	Diurnal temperature range	Annual mean difference between TX and TN	°C

[a] TN is daily minimum temperature.
[b] TX is daily maximum temperature.

where t is the year from 1960 to 2012; n_r is the number of stations in region r; $x_{i,t}$ is the index value of station i at year t in region r; and $x_{r,t}$ is the regionally averaged value at year t in region r.

The arithmetic mean was adopted to calculate the regional trends for six sub-regions in YRB:

$$S_{r,m} = \frac{1}{m}\sum_{i=1}^{m} S_{r,i} \tag{2}$$

where m is the number of stations in region r; $S_{r,i}$ is the slope magnitude of station i in region r; and $S_{r,m}$ is the regionally averaged trend in region r. One sample t-test (two tailed) was performed to test whether the regional trends ($S_{r,m}$) were significantly different from zero.

3.4. Low-pass filter

In order to highlight the decadal or longer time-scale variations and trends, the low-pass filter was applied to the annual anomaly series relative to 1961–1990 mean values for all temperature indices in this study. A detailed description of the filter computation can be found in chapter three of Climate change 2007: The Physical Science Basis wrote by Trenberth et al. (2007). Many previous studies also used similar filters to remove interannual or less than interdecadal variations of climate variables (Klein Tank et al., 2006; You et al., 2010b; Li et al., 2012b; Fu et al., 2013).

4. Results

4.1. Trends in statistical parameters of TN and TX

To understand how the extreme events changed in frequency and intensity, it is useful to first consider how such extremes could change in a statistical sense (Meehl et al., 2000). A change in the variance of extremes will have a greater impact on the frequency of the extremes than a change in the mean (Katz and Brown, 1992). In order to examine whether the variability of daily minimum temperature (TN) and daily maximum temperature (TX) changed over time, the trends in mean, variance, CV (coefficient of variance) and skewness of TN and TX during 1960–2012 were analyzed.

Annual mean values of both TN and TX increased with years in almost the whole YRB during 1960–2012, but the trends were stronger in TN than TX. These findings were consistent with the reports that TN increased more than TX, and were supported by You et al. (2008), Sang (2012) and Sang et al. (2012). For the whole YRB, significant upward trends of 0.24 and 0.15 °C/decade were detected in the mean values of TN and TX during 1960–2012 respectively, with 92% and 57% of stations showing statistically significant trends (Table 2). Geographically, six regions showed consistent significant warming. But warming was the most significant in region I (the eastern Tibet Plateau), where the largest magnitude of 0.33 and 0.21 °C/decade were detected in the mean values of TN and TX, respectively.

Contrary to mean value, the variance and CV decreased significantly in most parts of YRB, with more decreases occurring in TN than TX (Table 2). In other words, the mean temperature in YRB got warmer and warmer during the past 53 years but with smaller fluctuations, meaning that the lower temperatures (lower percentile of TN and TX) increased more than higher temperatures (higher percentile of TN and TX). For the YRB as a whole, the variance and CV of TN decreased significantly with a rate of −1.1 °C/decade and −0.04/decade respectively, with 45% and 85% of stations showing significant negative trends. Regionally, significant decreasing trends were observed in each of the six regions for both variance and CV of TN. The largest decrease was found in region I for variance (−1.49 °C/decade) and in region II (mid-western YRB) for CV (−0.13/decade). Compared with TN, the changing patterns of variance and CV for TX were of remarkably smaller magnitudes with fewer stations showing significant trends. Geographically, only region I and region IV (mid-eastern YRB) showed significant decreasing trends in variance of TX. The CV values of TX showed significant decreasing trends in all regions except region II.

The skewness of TN and TX showed very slight changes during 1960–2012, which were hardly detected. No significant trend was detected in skewness of TN for the whole basin (Table 2). Regionally, the only significant trend of 0.01/decade was observed in regions II and III (south-central YRB). For skewness of TX, a significant decreasing trend was detected for the whole YRB as well as regions IV, V (southeastern YRB) and VI (northeastern YRB).

4.2. Spatial distribution of extreme temperature indices

Fig. 2 depicts the spatial distribution of Mann-Kendall test for temperature indices at 143 meteorological stations during 1960–2012 in the YRB. The percentage of stations with downward and upward trend, and the regional trends for 15 indices in six regions as well as the whole YRB are shown in Tables 3 and 4 respectively. We describe results for each temperature index in turn.

All percentile indices, including TN10P, TN90P, TX10P and TX90P, displayed trends consistent with warming in most parts of YRB during 1960–2012, but the warming was stronger for indices derived from TN (e.g. TN10P and TN90P) than those from TX (TX10P and TX90P) (Fig. 2 and Table 4). The number of TN10P (TN90P) significantly decreased (increased) by a rate of −3.45 d/decade (2.95 d/decade) during 1960–2012, with 80% (62%) of stations showing significant downward (upward) trends (Tables 3 and 4). The regionally averaged trends were significant in all regions for both TN10P and TN90P except region IV for TN90P. In region I, TN10P (TN90P) exhibited a significant decreasing (increasing) trend of −4.85 d/decade (4.84 d/decade), the most significant warming for the two indices. It was noteworthy that there were several stations in region IV showing downward trends for

Table 2
Percentage of stations with downward and upward trend as well as trends per decade calculated for annually statistical parameters of TN and TX by region in the Yangtze River Basin during 1960–2012.

		Downward (%)	Upward (%)	Sen's slope of each variable in each region						
				I	II	III	IV	V	VI	YRB
Mean	TN	3	97 (92)	**0.33**[c]	**0.22**	**0.21**	**0.15**	**0.18**	**0.27**	**0.24**
	TX	4	96 (57)	**0.21**	**0.12**	**0.09**	**0.14**	**0.09**	**0.19**	**0.15**
Variance	TN	97 (45)[b]	3	**−1.49**	**−1.05**	**−0.65**	**−0.99**	**−0.84**	**−1.29**	**−1.10**
	TX	58 (1)	41(3)	**−0.45**	**0.64**	−0.04	**−0.44**	−0.14	0.02	−0.06
CV[a]	TN	97 (85)	3	**−0.07**	**−0.13**	**−0.02**	**−0.02**	**−0.01**	**−0.02**	**−0.04**
	TX	88 (23)	12	**−0.04**	0.01	**−0.01**	**−0.01**	**−0.01**	**−0.01**	**−0.01**
Skewness	TN	40 (2)	60 (4)	0	**0.01**	**0.01**	−0.01	−0.01	−0.01	0
	TX	66 (28)	34 (1)	0.01	−0.01	0.01	**−0.02**	**−0.02**	**−0.02**	**−0.01**

[a] CV is coefficient of variation.
[b] Values in the parentheses are the percentage of stations with that significant trend.
[c] Values in bold are significant trends (one sample T test) at the 5% level.

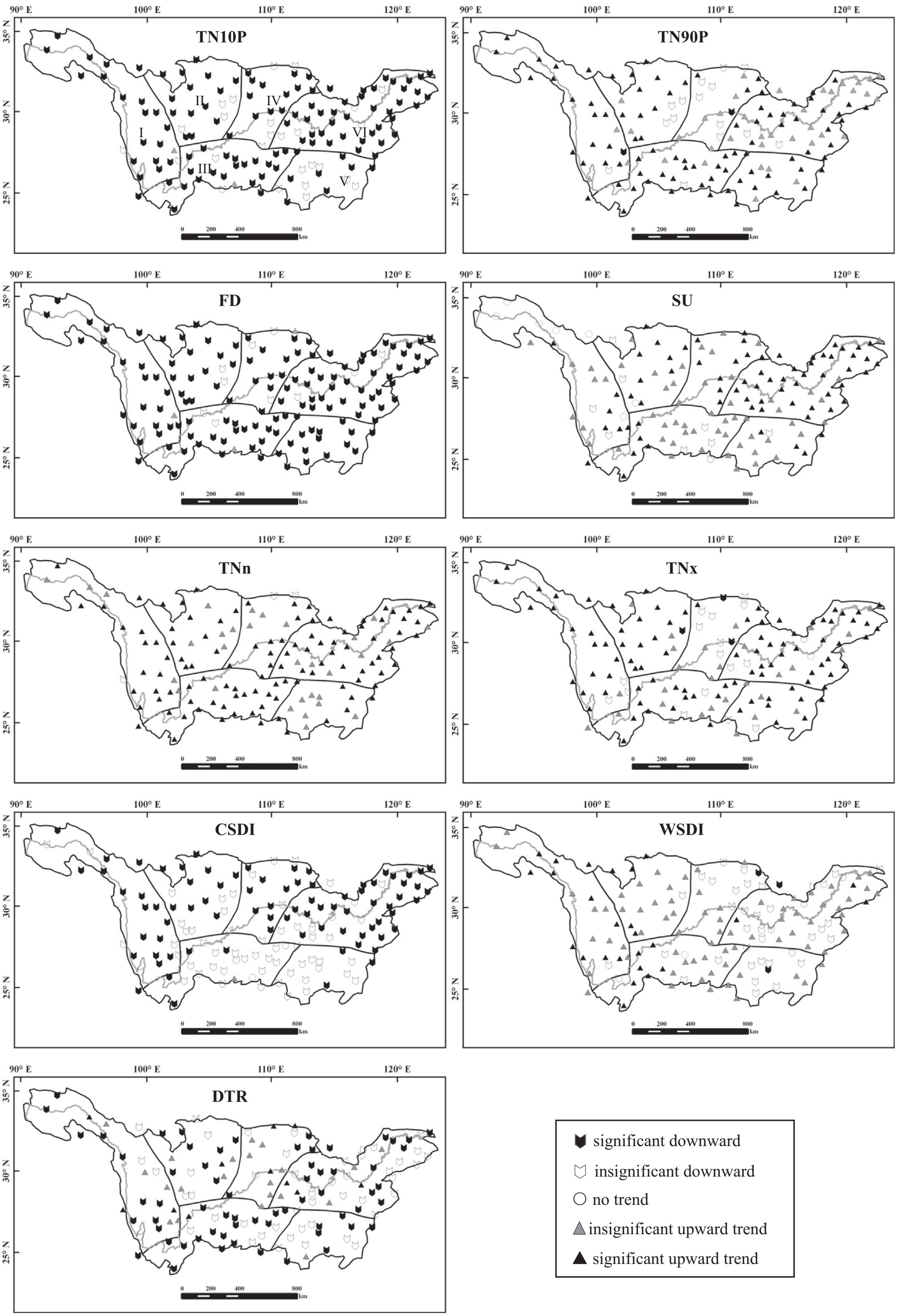

Fig. 2. Mann-Kendall trend test for temperature indices during 1960–2012 in the Yangtze River Basin. ⬇ denotes the significant downward trend, ▽ denotes the insignificant downward trend, ○ denotes no trend, △ denotes the insignificant upward trend, ▲ denotes the significant upward trend.

Table 3
Percentage of stations with downward and upward trends calculated for temperature indices using Mann-Kendall test in the Yangtze River Basin during 1960–2012.

Index	Downward (%)	Upward (%)
TN10P	99 (80)[a]	1
TN90P	12 (1)	88 (62)
TX10P	73 (23)	27
TX90P	21 (1)	78 (30)
FD	98 (91)	2
SU	6	89 (50)
ID	83 (22)	4
TR	10 (1)	59 (33)
TNn	2	98 (76)
TNx	14 (2)	85 (65)
TXn	5	95 (35)
TXx	19	81 (30)
CSDI	99 (57)	1
WSDI	30 (2)	69 (18)
DTR	78 (45)	22 (7)

[a] Values in the parentheses are the percentage of stations with that significant trend.

TN90P though most of them were insignificant. The spatial patterns of TX10P (TX90P) were similar to those of TN10P (TN90P) to some extent, but with smaller magnitudes and fewer stations showing significant trends. It should be noted that stations with significant trends occurred mostly in region I, where the largest significant decrease (increase) of −2.95 d/decade (3.48 d/decade) was detected, more than doubling the trends in the whole YRB.

The number of FD demonstrated a significant decreasing trend of −3.04 d/decade for the YRB, with 91% of stations showing significant downward trends (Tables 3 and 4). The regional trends for FD were all significant in each of the six regions, ranging from −4.38 d/decade in region I to −1.70 d/decade in region V. Alexander et al. (2006) analyzed the global changes in climate extremes of daily temperature, and concluded that the largest significant change for FD appeared in the Tibet Plateau, which was consistent with the results in this study. In comparison with FD, ID showed a remarkably smaller magnitude of −0.42 d/decade and fewer stations (22%) with significant trends in the YRB. The strongest warming again occurred in region I where the only significant decrease of −1.75 d/decade was observed. Inversely, SU and TR showed a significant increasing trend of 2.16 and 1.05 d/decade over the whole YRB. The percentages of stations with significant positive trends were 50% and 33%, respectively. Geographically, the greatest magnitude for SU was found in region VI at a rate of 3.12 d/decade. For TR, almost all stations had no trends in region I and its surrounding areas due to the low temperatures and high elevations. And thus the more significant increasing trends of 2.54 and 1.95 d/decade were found in regions V and VI. Moreover, it was worthwhile to note that 50% (data not shown) of stations in region IV showed downward trends, which was inconsistent with the warming in most stations.

The absolute indices of TNn, TNx, TXn and TXx exhibited significant warming for the whole YRB during 1960–2012. However both the magnitudes and number of stations with significant trends were larger for TNn and TNx than for TXn and TXx (Table 4). For the YRB as a whole, TNn and TXn significantly increased with a trend of 0.42 and 0.28 °C/decade respectively, with approximately 76% and 35% of stations showing significant increasing trends (Tables 3 and 4). The regional trends for TNn and TXn were all significant in all regions except region II for TXn. Stations in region VI had the largest magnitudes of 0.48 and 0.34 °C/decade for TNn and TXn respectively, indicating more rapid warming in this region. TNx displayed very similar patterns to TNn, but of smaller magnitudes in all regions. The smallest trend for TNx was found in region IV where an insignificant trend of 0.03 °C/decade was observed. For TXx, the whole YRB exhibited a significant increasing trend of 0.14 °C/decade, and the percentage of stations showing significant positive trends was about 30%. With the exception of regions IV and V, significant warming was detected in other regions. Greater magnitudes occurred in regions I and II at the trends of 0.22 and 0.25 °C/decade respectively.

The annual occurrence of CSDI significantly decreased at a rate of −1.6 d/decade for the whole YRB, with 57% of stations passing the significance test (Tables 3 and 4). Regionally, the decreasing trends in all six regions were significant with region I being the greatest at −2.02 d/decade and region V the least at −0.90 d/decade. Compared with CSDI, the WSDI trends were less consistent throughout regions. Overall, the WSDI significantly increased with a trend of 0.73 d/decade for the YRB. Stations with significant increasing trends mainly distributed in regions I, II and III.

For DTR, 45% of stations showed significant downward trends, while 7% showed significant upward trends in YRB (Table 3). The whole YRB exhibited a significant decreasing trend of −0.09 °C/decade, indicating greater warming in TN than in TX (Table 4). Geographically, DTR decreased significantly in all regions but region IV, where the most stations with increasing trends were found. The greatest magnitude of −0.11 °C/decade was observed in region I.

Table 4
Trends in days or °C per decade for temperature indices using Sen's slope estimator in six regions of the Yangtze River Basin during1960–1985, 1986–2012 and 1960–2012.

Time period	Region	Index														
		TN10p	TN90p	TX10P	TX90p	FD	SU	ID	TR	TNn	TNx	TXn	TXx	CSDI	WSDI	DTR
1960–1985	I	**−3.85**[a]	−0.28	**1.97**	−0.68	**−1.74**	0.67	0.30	[b]	**0.38**	−0.01	**−0.25**	**0.19**	**−2.37**	0.11	**−0.27**
	II	−0.90	**−2.36**	**2.71**	**−3.73**	−0.76	**−2.76**	0.18	−0.61	**0.39**	−0.12	**−0.38**	−0.10	0.12	**−0.90**	**−0.26**
	III	−0.64	**3.32**	**2.60**	**−2.85**	−0.29	**−2.19**	**0.44**	0.71	**0.32**	**0.24**	**−0.33**	**−0.25**	**2.30**	**−1.37**	**−0.30**
	IV	**1.49**	**−2.57**	**3.13**	**−5.83**	0.61	**−2.56**	**0.20**	**−1.50**	0.20	**−0.22**	**−0.43**	**−0.38**	**0.84**	**−4.08**	**−0.27**
	V	0.69	**3.72**	**3.88**	**−5.43**	−0.04	**−3.74**	0.18	**2.44**	**0.36**	**0.16**	**−0.26**	**−0.36**	**2.15**	**−4.70**	**−0.39**
	VI	−0.29	**−1.77**	**3.97**	**−4.89**	−0.66	**−2.47**	0.01	**−1.65**	**0.34**	−0.07	**−0.24**	**−0.29**	**−0.94**	**−4.87**	**−0.33**
	YRB	**−0.53**	−0.24	**3.13**	**−3.89**	−0.56	**−2.18**	0.21	−0.12	**0.32**	−0.01	**−0.31**	**−0.20**	0.08	**−2.84**	**−0.31**
1986–2012	I	**−4.61**	**8.45**	**−5.78**	**8.48**	**−5.87**	**4.49**	**−2.46**	-	**0.49**	**0.28**	**0.69**	**0.20**	**−4.00**	**4.78**	0.08
	II	**−3.14**	**6.67**	−0.52	**6.84**	**−2.93**	**5.82**	−0.54	**1.75**	**0.16**	**0.47**	0.05	**0.61**	**−2.90**	**6.05**	0.01
	III	0.04	**8.10**	0.19	**7.85**	−0.46	**7.24**	−0.02	**1.68**	**0.21**	**0.20**	**0.17**	**0.38**	**−0.90**	**5.24**	0.01
	IV	**−1.42**	**7.42**	−1.19	**6.33**	**−2.71**	**5.73**	0.40	**2.65**	−0.11	**0.30**	**0.23**	**0.51**	**−3.00**	**3.99**	0.10
	V	0.99	**6.99**	−0.16	**7.54**	0.20	**7.69**	0.20	**5.54**	−0.12	**0.37**	0.02	**0.32**	**−1.00**	**6.41**	0.05
	VI	−0.20	**8.18**	−0.10	**7.25**	−0.48	**8.51**	**−0.47**	**6.16**	−0.09	**0.48**	0.04	**0.27**	**−3.80**	**4.90**	0.01
	YRB	−1.27	**7.80**	−1.26	**7.41**	**−1.86**	**6.87**	−0.49	**3.56**	0.08	**0.36**	0.19	**0.36**	**−2.70**	**5.13**	0.04
1960–2012	I	**−4.85**	**4.84**	**−2.95**	**3.48**	**−4.38**	1.34	**−1.75**	-	**0.46**	**0.21**	**0.21**	**0.22**	**−2.02**	**2.16**	**−0.11**
	II	**−3.55**	**2.20**	**−1.00**	**2.24**	**−2.66**	**1.70**	−0.02	0.68	**0.39**	**0.19**	0.16	**0.25**	**−1.53**	**1.25**	**−0.09**
	III	**−3.03**	**4.03**	**−0.65**	**1.95**	**−2.49**	**1.63**	−0.47	0.32	**0.45**	**0.16**	**0.31**	**0.13**	**−0.94**	**0.89**	**−0.10**
	IV	**−2.73**	0.92	**−0.88**	0.40	**−2.50**	**2.31**	−0.09	0.20	**0.29**	0.03	**0.31**	0.03	**−1.72**	0.02	0.02
	V	**−2.19**	**3.42**	**−0.08**	0.14	**−1.70**	**1.87**	−0.11	**2.54**	**0.31**	**0.14**	**0.30**	0.04	**−0.90**	−0.45	**−0.09**
	VI	**−3.63**	**2.32**	**−0.63**	**1.51**	**−3.49**	**3.12**	−0.19	**1.95**	**0.48**	**0.25**	**0.34**	**0.14**	**−1.98**	0.51	**−0.08**
	YRB	**−3.45**	**2.95**	**−1.03**	**1.71**	**−3.04**	**2.16**	**−0.42**	**1.05**	**0.42**	**0.18**	**0.28**	**0.14**	**−1.60**	**0.73**	**−0.09**

[a] Values in bold are significant (one sample T test) at the 5% level.
[b] Annual mean temperature in region 1 (eastern Tibet plateau) is quite low and TR is rare in a year, so it is not included in the calculation.

Overall, the most significant warming was found in region I in most cases during 1960–2012 (Table 4). These characteristics further indicated the topography effects on warming as confirmed by Pepin and Seidel (2005) and Li et al. (2012b). Besides, many previous studies suggested that the warming was more prominent at higher elevations than lower elevations (Beniston and Rebetez, 1996; Diaz and Bradley, 1997; Beniston, 2003; Liu et al., 2009; Li et al., 2011b; Wang et al., 2013b). Whether the warming rates in temperature extremes increased with altitude in YRB would be discussed in Section 5.2. In addition, the greatest warming was also detected in region VI for several indices like SU, TNn, TNx and TXn during 1960–2012(Table 4).

While most stations in YRB showed warming trends during 1960–2012, several stations mainly located in region IV did show cooling trends though insignificant (Fig. 2). As shown in Table 4, TN90P, TX90P, TR, WSDI, TNx and TXx exhibited the smallest insignificant warming rates of 0.92, 0.40, 0.20, 0.02 days/decade, and 0.03 and 0.03 °C/decade respectively in region IV, which was not completely consistent with the general warming in YRB. This reflected the instability and complexity of climate change in a large river basin under the background of global change. Such finding was confirmed by many studies at the Hengduan Mountain (Li et al., 2011b), in Sichuan Province, China (Wang et al., 2013b) and Southwest China (Li et al., 2012b).

4.3. Temporal changes of extreme temperature indices

4.3.1. Temporal variations in annual time series anomalies for entire basin

Commonly it is of great interest to produce one single time series to represent a region in order to summarize the temporal variations in climate extremes. The above results provided limited information regarding the interannual or longer time-scale variability in temperature indices. Hence, insight into this variability was provided in this section. For each index, the time series anomalies were calculated by averaging 143 stations in YRB, and then subtracted the 1961–1990 mean values. As shown in Fig. 3, almost all temperature indices showed an obviously warming trend although with small fluctuations during 1960–2012. The year 1985 was a turning point for several indices like TN10P, FD, ID, TNn, TXn and CSDI transiting from relatively cold period to warm period. This is exactly why we chose 1985 to split the entire period for more detailed trend analysis in Section 4.3.3.

For percentile indices, TN10P, TN90P and TX90P all experienced significant warming except TX10P. But the warming was more pronounced in TN10P and TN90P, indicating the greater warming at nighttime than daytime. TN10P showed a general decreasing trend during 1960–2012. The decreasing trend became more evident after mid-1980s, indicating an accelerated warming. The warmest year for TN10P occurred in 2007, with about 21 cold nights fewer than the mean value in 1961–1990. The variation of TX10P exhibited neither a stable nor a gradual pattern during 1960–2012, and there were several cold and warm periods throughout 1960–2012. The temporal variations of TN90P and TX90P were basically the same. Both of them showed a general increasing trend during 1960–2012, which became increasingly clear after 2000.

The anomaly series of FD and ID, compared with the 1961–1990 averages, were generally positive before the mid-1980s but negative thereafter. But overall they showed a pronounced decreasing trend during 1960–2012. The coldest year after 1985 occurred in 2008 for both FD and ID, which was 0.9 and 3.4 days greater than the 1961–1990 mean values, respectively. The indices of SU and TR exhibited general decreasing trends before mid-1970s and increasing trend since 1990 which became more evident after 2000. Meanwhile, the coldest year after 2005 also occurred in 2008 for the two indices.

All the absolute indices displayed synchronized warming in YRB. From 1960 to late-1970s, the anomalies of TNn were mostly lower than the 1961–1990 mean value and showed no obvious changes, but TXn exhibited a decreasing trend. Besides, eight years were ranked among the ten coldest years in the anomaly series for both TNn and TXn during 1960–1977. After late-1970s, both TNn and TXn anomalies displayed a pronounced warming trend. TNx displayed a slightly declining trend before early-1970s, whereas a clear increasing trend occurred after mid-1980s and more rapid increase took place after 2000. For TXx, no significant changes were detected in 1960s, but a decreasing trend exhibited during 1970s and early-1980s, and then followed by an increasing trend. Furthermore, it is worthwhile to note that the minimum anomaly after 2000 appeared in 2008 for all the absolute indices. As indicated by Gao (2009), South China endured record cold temperatures in winter 2008 because of an unprecedented persistent rain, snow and ice storms during January and February 2008. The causes of the snow disasters in 2008 were ascribed to the anomalous circulation in the high latitudes and the La Nina event began in 2007 (Gao, 2009).

Obviously, the anomaly series of CSDI were mostly dominated by positive values in 1960–1985, and eight years were ranked among the ten coldest years. However, the anomaly values after 1985 were all below the 1961–1990 average except for 1993, 2008 and 2011. These characteristics indicated that there was a general decreasing trend for the entire period. WSDI showed a decreasing trend before 1985 and a rapid increase afterwards. As for DTR, the temporal variations displayed a decreasing trend before early-1980s, followed by an unexpected path, with an increasing trend from 1990 to 2005 which was interrupted by a rise up to the most recent period (2012).

4.3.2. Temporal variations of Mann-Kendall test in six sub-regions

The above analysis gave an overall picture of the whole YRB. It is not a good representation of the actual change in each region because the YRB displays a wide variety of climate zones owing to the topographical complexity and three types of monsoons. Moreover, we had no idea whether the changes were significant or not from the statistical point of view. For each index, the non-parametric Mann-Kendall test was therefore performed on the time series of six regions as well as the whole YRB to further examine the temporal changes of temperature indices during 1960–2012. The results (Fig. 4) were mostly consistent with those obtained in the previous sections.

Overall TN10P displayed more pronounced warming than other percentile indices during 1960–2012. Geographically, region I exhibited a decreasing trend since the mid-1960s and the decreasing trend became significant around early-1980s. However, the other regions as well as the whole YRB showed a decreasing trend since the early-1980s, which became statistically significant after 1990 in these regions. This further confirmed the findings that region I experienced more rapid warming during 1960–2012. The warming patterns of TX10P were not exactly the same as TN10P. TX10P displayed a decreasing trend since late-1980s in all regions, but the only significant decreasing trend was observed in region I. TN90P showed a decreasing trend from 1960 to mid-1970s for the YRB as a whole, and then an increasing trend after 1990s that became significant around 2006. The similar changes were exhibited in regions I and III, but significant warming was found around 1997 for both regions. The warming trends for regions II, V and VI became significant in late-2000s. The number of TX90P showed very similar patterns to TN90P. But significant warming was only detected in regions I, II and III after 2006.

For the threshold indices, the changing patterns of FD and ID, to a large extent, were very similar to those of TN10P. The only difference was that significant decreasing trends occurred around 1990 and 2000 in most regions. The number of SU decreased from early-1960s to early-1990s in most regions, and increased afterwards. The increasing trends became significant around mid-2000s for all regions. The changing patterns for TR showed more regional differences. Overall, a decreasing trend was found in all regions during 1960s and late-1970s with region V being significant. Afterwards, increasing trends began around 1980 in regions III and V and around 2000 in the whole basin and region VI, and became significant around 2008. Regions II and IV exhibited a continuously insignificantly decreasing trend before mid-2000s, but an increasing trend afterwards though insignificant. In region I, TR is very rare in a year due to the low temperature, so it is not included in the calculation.

As for the absolute indices, warming trends for TNn and TNx were generally more significant than TXn and TXx. For TNn, the whole YRB and regions I, II and V generally showed increasing trends during 1960–2012, which became significant between mid-1980s and late-1990s. Regions III, IV and VI largely showed decreasing trends before 1980 and then increasing trends that became significant

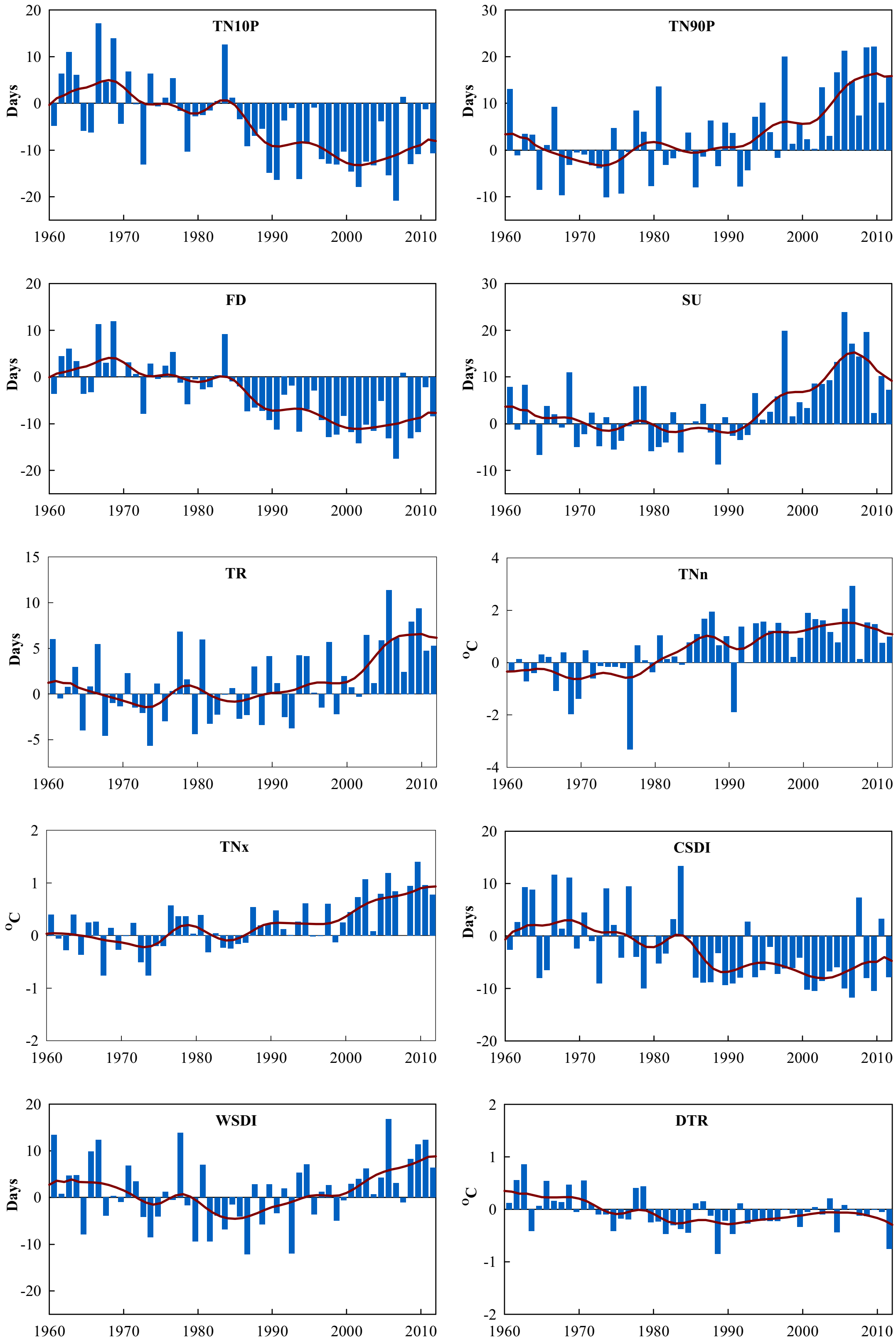

Fig. 3. Annual anomaly series relative to 1961–1990 mean values for temperature indices during 1960–2012 in the Yangtze River Basin. The bold solid lines are time series being smoothed by a low-pass filter (Trenberth et al., 2007).

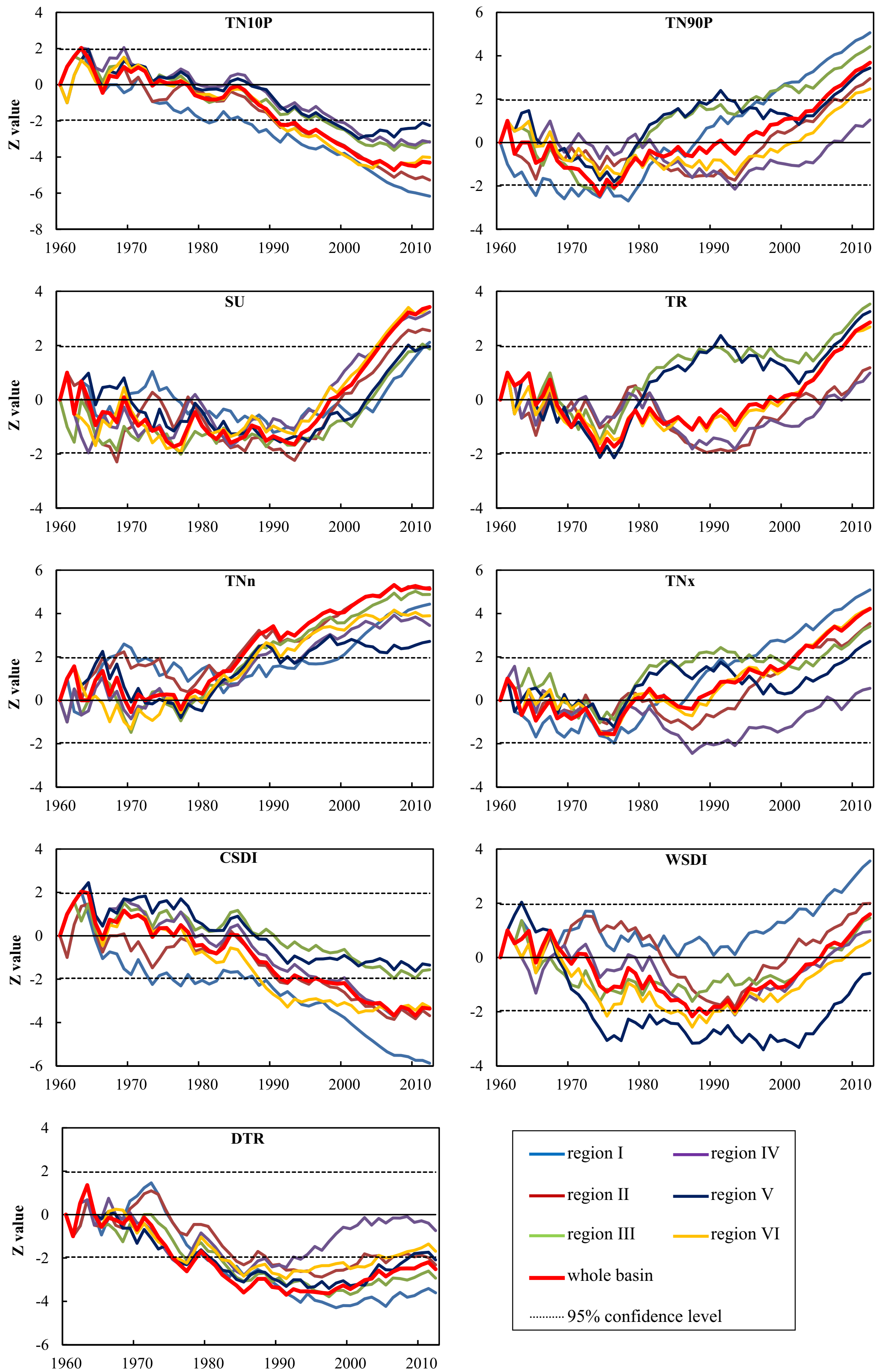

Fig. 4. Temporal changes of MK test Z-value of temperature indices in six regions of the Yangtze River Basin during 1960–2012. Annual mean temperature in region I is quite low and TR is rare in a year, so it is not included in the calculation.

around late-1980s. TXn exhibited similar changing patterns with TNn. The difference was that significant warming for TXn occurred later for most regions. As for TNx, decreasing trends were observed for all regions before late-1970s. Afterwards general increasing trends began in all regions but IV, where the decreasing trend continued to 2010 but was significant only around 1990. The increasing trend became significant in mid-1990s for region I, around 2000 for regions II and VI, around 1990 and again in mid-2000s for region III, and around 2010 for region V. The changing patterns of TXx were more or less the same as TNx, but significant warming was only detected in regions I, II and VI besides the YRB as a whole.

CSDI displayed consistently decreasing trends since mid-1960s in regions I and II. The decreasing trend was first found significant around mid-1970s for region I and in mid-1990s for region II, and the significance increased substantially by 2012. The increasing trends though insignificant were shown before 1980 for regions IV and VI and the whole basin, and before late-1980s for regions III and V, with the decreasing trends followed afterwards. The decreasing trend became significant around 1990 for region VI and the whole basin, and in mid-1990s for region IV. For regions III and V, the decreasing trends were persistent but never became significant by 2012. WSDI showed decreasing trends between 1970 and mid-2000s for all regions but I and II, and the decreasing trends were significant only for regions V and VI. Region I showed a consistent increasing trend during 1960–2012, which became significant around 2005. Region II exhibited increasing trends before mid-1980s and after 2000 that became significant around 2010.The recent increasing trends in regions III, IV and VI would become significant in the next several years if the warming trends continue.

The MK series of DTR was consistent with the anomaly series presented in last section. DTR displayed general decreasing trends in all regions for almost the entire period. The decreasing trends became significant between late-1970s and mid-2000s for all regions except region IV.

4.3.3. Temporal variations of temperature indices during1960–1985 and 1986–2012

To further investigate whether there is a change in the variations of temperature extremes between the two periods, the trends and variability of the fifteen temperature indices during 1960–1985 and 1986–2012 are compared in this section. The regional trends of all indices in six regions as well as the whole YRB during the two periods are shown in Table 4. Fig. 5 illustrates the percentages of stations with downward and upward trends for several representative indices in YRB and six regions as well.

For the whole basin, TN10P showed a significant downward trend at −0.53 d/decade during the first period of 1960–1985, and an insignificant trend at −1.27 d/decade during the second period of 1986–2012 (Table 4). The regional trends were more mixed in 1960–1985, but in 1986–2012 significant downward trends were found in regions I, II and IV. Overall, compared with 1960–1985, the percentages of significant downward trends increased in 1986–2012 for the whole basin as well as most regions, but the percentages of insignificant upward trends decreased for most regions (Fig. 5). TN90P did not exhibit a consistent trend across the whole YRB during 1960–1985, with many neighboring stations showing opposite trends. However, a significant upward trend of 7.8 d/decade was detected for the whole basin during 1986–2012,

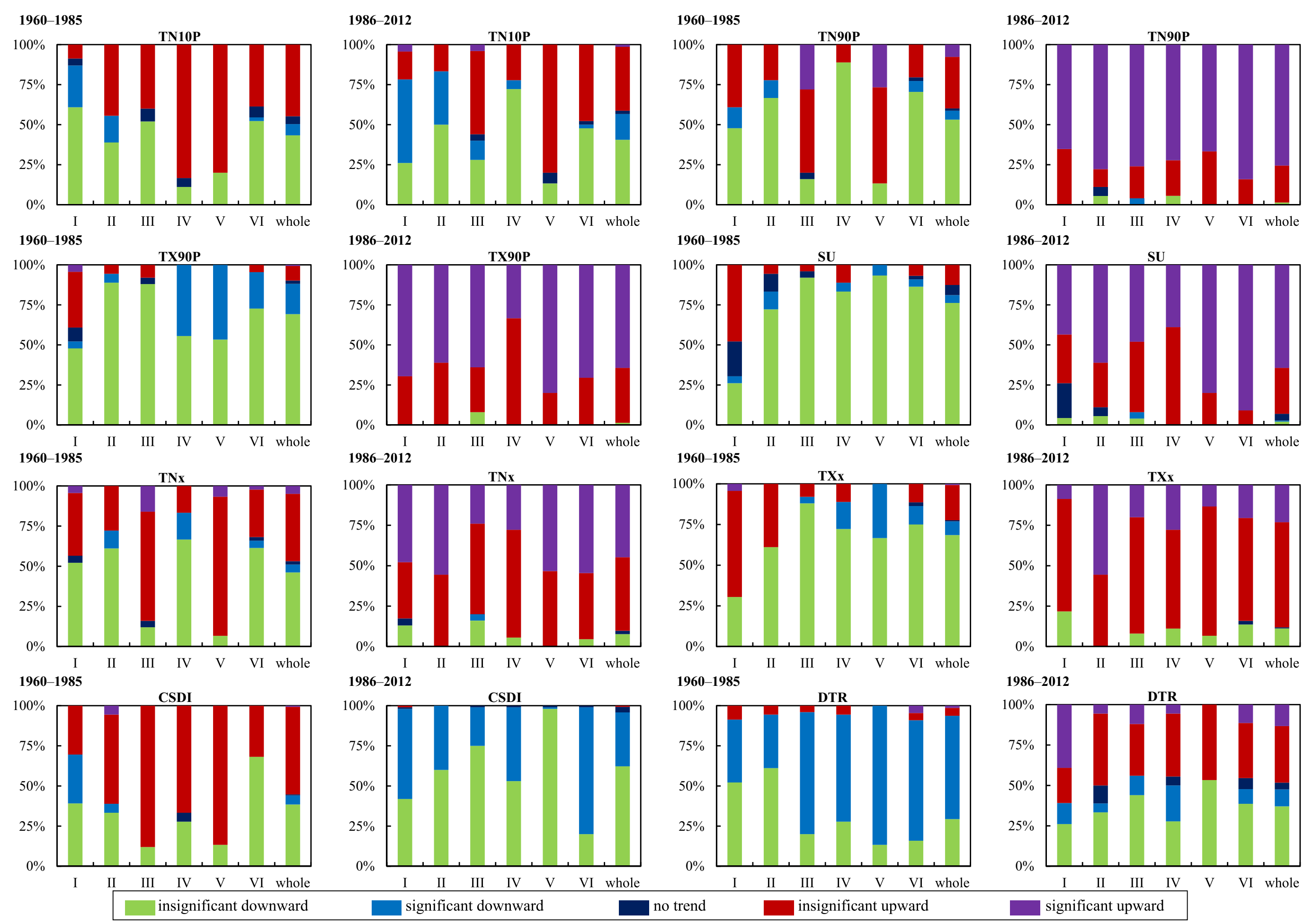

Fig. 5. Percentage of stations with downward and upward trends calculated for temperature indices in six sub-regions of the Yangtze River Basin during 1960–1985 and 1986–2012.

and the regional increasing trends were all significant (Table 4), indicating an accelerated warming after mid-1980s. As for TX10P, all regions showed significant increasing trends during 1960–1985, whereas most regions displayed insignificant decreasing trends during 1986–2012 except for region I where significant decreasing trend was detected (Table 4). This indicated a cooling period before mid-1980s for TX10P. The changing trends of TX90P during the two periods were totally opposite. During 1960–1985, significant decreasing trends were detected for all regions but region I. However, significant increasing trends were detected for all regions during 1986–2012, especially in region I where the greatest increase was observed (Table 4). Compared with 1960–1985, the percentages of all downward trends (significant plus insignificant) decreased while the percentages of all upward trends increased during 1986–2012 (Fig. 5), again confirming a cooling period before 1985 and a warming period afterwards.

For FD, the trend patterns were generally more mixed during 1960–1985 and no significant changes was detected for the YRB as a whole (Table 4). During 1986–2012, FD significantly decreased at −1.86 d/decade for the whole basin. Obviously, the percentages of significant downward trends increased during 1986–2012 compared with 1960–1985, especially in regions I and II (Fig. 5). For SU, there were opposite trends between the two periods, but synchronous trends existed within each period. All regions but region I showed significant decreasing trends during 1960–1985, while all regions displayed significant increasing trends during 1986–2012 (Table 4). Compared with 1960–1985, the percentages of all downward trends decreased while those of all upward trends increased during 1986–2012 (Fig. 5). As for ID, increasing trends were observed for all regions during 1960–1985 though only regions III and IV were significant (Table 4). Four regions showed decreasing trends during 1986–2012 with regions I and VI being significant. The trend patterns for TR were mixed during 1960–1985, but TR significantly increased in all regions during 1986–2012. These characteristics all indicated an accelerated warming after mid-1980s in YRB.

Apparently, TNn displayed a significant warming trend of 0.32 °C/decade for the whole YRB during 1960–1985 (Table 4). Regionally, all regions but IV showed upward trends at more than 70% of stations (Fig. 5). During 1986–2012, the warming trends subsided in most regions with regions I, II and III still being significant. For TNx, the trends were mixed during 1960–1985, and thus no significant trend was observed for the whole basin (Table 4). During 1986–2012, TNx showed spatially consistent warming with a significant increasing trend of 0.36 °C/decade in the whole basin. The regional trends were significant in all regions, with more than 83% of stations showing increasing trends (Table 4 and Fig. 5). Compared with 1960–1985, all upward trends increased while all downward trends decreased in all regions during 1986–2012(Fig. 5). For TXn, all regions displayed significant downward trends during 1960–1985, and upward trends during 1986–2012 with regions I, III, and IV being significant (Table 4). During 1960–1985, TXx showed significant downward trends in regions III-VI. During 1986–2012, all regions displayed significant upward trends. In general, the percentages of downward trends decreased while those of upward trends increased in all regions compared with 1960–1985 (Fig. 5).

As for CSDI, upward trends were mainly detected in regions II-V, and downward trends were mainly observed in regions I and VI during 1960–1985(Fig. 5). During 1986–2012, the whole basin exhibited a significant warming trend of −2.7 d/decade for CSDI. 96% of stations were in decreasing trends and 34% of stations passed the significance test. The regional trends were all significantly decreased, with the most decrease occurring in regions I (Table 4). Compared with 1960–1985, the percentages of upward trends decreased while those of downward trends increased in all regions during 1986–2012(Fig. 5). The changing patterns of WSDI were completely opposite between the two periods, but very similar to those of SU. In general, all upward trends increased while all downward trends decreased in all regions during 1986–2012. From the above results, we can conclude that significant warming occurred especially during 1986–2012 for both CSDI and WSDI in the basin.

From the spatial distribution of DTR, it could be seen that 94% of stations showed decreasing trends in YRB during 1960–1985, and 64% of stations were significant (Fig. 5). The results also indicated that DTR exhibited a significant decreasing trend of −0.31 °C/decade in the whole basin (Table 4). Geographically, the regionally averaged trends were all significantly decreased. During 1986–2012, DTR did not exhibit a consistent and significant trend across the whole YRB, with many neighboring stations showing opposite trends. All regions showed positive trends but none was significant.

Generally speaking, differences in the variations of temperature indices were definitely noticeable between 1960–1985 and 1986–2012 (Table 4, Figs. 3, 4 and 5). Our findings pointed to strong warming especially after the mid-1980s, which were in line with the trends in the Tibetan Plateau (Kang et al., 2010), at the Hengduan Mountains (Li et al., 2011b) and in the Yangtze River Delta (Sang, 2012). During 1960–1985, the trends in temperature indices were more ambiguous compared with those during 1986–2012 (Table 4). But most temperature indices showed cooling trends for the whole YRB, and statistically significant cooling trends were detected in TX10P, TX90P, SU, TXn, TXx and WSDI. It is noteworthy that region I already started to show significant warming in several indices like TN10P, FD, TNn, TXx and CSDI during 1960–1985 (Table 4). During 1986–2012, the warming trends were pronounced especially in the warm-related indices such as TN90P, TX90P, SU, TR, TNx, TXx and WSDI, more than doubling the changes in 1960–2012. This confirmed that there was a cooling period before the mid-1980s but an accelerated warming thereafter in most cases. This finding was similar to Li et al. (1995) who indicated that Sichuan Basin showed a cooling trend from the 1960s to mid-1990s. It should be mentioned that several indices like TN10P, FD and ID did not exhibit spatially coherent trends across the whole YRB in both periods. This was because the time series in both periods were not long enough to allow the detection of reliable trends, as evidenced by the detection of more coherent trends in YRB during the entire period of 1960–2012.

5. Discussion

5.1. Comparisons with previous studies

Trends and variability analyses of daily temperature extremes in YRB during 1960–2012 revealed widespread significant changes associated with warming over most of the regions analyzed, and the warming trends were greater in the minimum temperature indices than the maximum temperature indices (Fig. 2 and Table 4). These findings were in line with many previous studies at a regional or national scale around the world (Peterson et al., 2002; Klein Tank and Können, 2003; Zhang et al., 2005b; Alexander et al., 2006; Klein Tank et al., 2006; You et al., 2011; Li et al., 2012a, 2012b; Skansi et al., 2013; Wang et al., 2013a, 2013c, 2014; Liang et al., 2014). Based on the same suite of temperature indices as defined by ETCCDI, the regional trends of this study were largely similar to those reported by Wang et al. (2014). The small differences were mainly due to the differences in meteorological station distribution or trend computation methods. Besides, warming in temperature extremes is stronger in YRB than in the Southwestern China (Li et al., 2012b), but weaker than the Central and eastern Tibetan Plateau (You et al., 2008).

According to Zhang et al. (2005b), Alexander et al. (2006), Klein Tank et al. (2006), IPCC (2007), You et al. (2011), Skansi et al. (2013) and Liang et al. (2014), there have been significant decreasing trends of DTR because of the faster warming in minimum temperature than maximum temperature. However, the DTR variability in YRB was not completely consistent with the above results. While most regions showed significant decreasing trends for DTR during 1960–2012, region IV showed an increasing trend of 0.02 °C/decade though insignificant

(Table 4), as those found in Central America and northern South America (Aguilar et al., 2005). Besides, it is worth to note that the decreasing trends in DTR all occurred in the first period (Table 4). However, in 1986–2012, DTR showed increasing trends though insignificant in all sub-regions and the whole YRB. This corroborates the finding of Sang (2012) who indicated that DTR shows a positive trend in the mid and southern Yangtze River Delta during 1986–2007. Vose et al. (2005) conducted a thoroughly analysis of DTR changes at a global scale, concluding that the widespread decrease of DTR was only evident from 1950–1980. Then Rohde et al. (2013) and Wild et al. (2007) noted an apparent reversal since the mid-1980s with DTR subsequently increasing over global land surfaces. The DTR variability is determined by the variability of both TN and TX (TX minus TN). During 1986–2012, the increasing magnitudes of TXn and TXx are stronger than those of TNn and TNx in almost all regions of YRB (Table 4). Therefore, the increasing trend in DTR is mainly due to the relatively bigger increase of TX than TN during 1986–2012. As indicated by Rohde et al. (2013), this change in direction is unexpected and not anticipated by existing climate models. The fifth assessment of IPCC pointed out that the decrease and subsequent increase in DTR is consistent with the dimming and subsequent brightening (IPCC, 2013). Sang (2012) associated the DTR increase with urbanization impacts. Changes in precipitation, soil moisture and atmospheric circulation likely accounted for DTR variation (Vose et al., 2005). However, these reasons cannot completely explain the DTR changes in YRB. Currently, there is no consensus about the physical reasons of DTR changes, especially DTR increase. Further studies are needed to address this issue.

5.2. Possible causes of observed changes in temperature extremes

The whole YRB experienced widespread significant warming during the past 53 years, especially in eastern Tibet Plateau (region I) and northeastern YRB (region VI). Kang et al. (2010) suggested that the warming in the Tibet Plateau would continue in phase with global trends, but in a greater magnitude. Based on the modeling results presented in previous studies, the increasing anthropogenic greenhouse gases are generally considered as the major cause of the warming in the YRB (Liu and Chen, 2000; Chen et al., 2003; Duan et al., 2006; IPCC, 2007). However, other confounding factors, such as changes in cloud cover, Asian brown clouds and land uses may also contribute to recent warming (Frauenfeld et al., 2005; Duan and Wu, 2006; Ramanathan et al., 2007; Zhang, 2007). The snow and ice-albedo feedback is regarded as another factor in the Tibet Plateau, which is one of the most sensitive and susceptible areas to snow feedback on the Earth (Liu and Chen, 2000). Besides, many studies demonstrate that atmospheric circulation change is an important mechanism affecting the heat and moisture transportation in this region (Zhang et al., 2007, 2008; You et al., 2008, 2011; Li et al., 2012a; Wang et al., 2013a). During summer, the subtropical high pressure or anticyclone tends to be enhanced over southern China, which plays an important role in increasing occurrences of extremely high temperature days in YRB (You et al., 2011; Li et al., 2012a). In winter, the southwesterly wind has strengthened, and consequently weakens the southern extent of Siberian northwest monsoon and limits the southward extension of cold flow (You et al., 2011). This would explain why the cold-related indices significantly decreased in the YRB. However, the exact impacts of these factors on warming will need further investigation.

In addition, it should be pointed out that the contribution of urban heat island (UHI) effect to warming trends in global temperature records cannot be ignored (IPCC, 2007). Sang et al. (2012) indicated that daily minimum, mean and maximum temperature showed more notably increasing trends after the 1980s especially in the Yangtze River Delta than the surrounding areas due to the UHI effects, as similarly reported by He et al. (2006), Du et al. (2007) and Xie et al. (2010). However, IPCC (2007) suggested that UHI effects are real but local, and have not biased the large-scale trends. If a certain basin or region has a large area and extremely rugged topography, such as the YRB considered here, the urbanization impacts cannot be easily detected (Sang et al., 2012). Therefore, the UHI effects should be studied in depth at various regional scales.

Elevation dependency of climatic warming is a very interesting phenomenon found in previous studies (Beniston and Rebetez, 1996; Liu et al., 2009; You et al., 2010a; Wang et al., 2013b). At present, there is no report on elevation dependency of temperature changes in YRB. Table 5 shows the relationships between trend magnitudes at individual stations and elevations for each temperature index in the YRB during 1960–2012. When elevation was below (above) 350 m, ID (TR) was not included in the calculation due to the low occurrences of the events. As a whole, most temperature indices indicated strong relationships between trend magnitudes and elevation. When elevation was above 350 m, significantly negative correlations were found for cold-related indices such as TN10P, TX10P, FD, ID, CSDI and DTR but the opposite was true for TN90P, TNn, and TNx. This suggested that the warming trends of these indices increased with increasing altitude in YRB, in accordance with other studies in Switzerland (Beniston and Rebetez, 1996), over the Rocky Mountains during winter and spring (Fyfe and Flato, 1999), in Mountain Qomolangma region (Yang et al., 2006), and in European Alps region (Giorgi et al., 1997). Besides, the warming rates for most indices were the largest at relatively higher elevations (1800–3200 above sea levels). This corroborated the result of Wang et al. (2013b) who found that the warming was more prominent at higher elevations (2000–3000 m a.s.l.) in Sichuan Province, Southwestern China. Liu et al. (2009) also found the elevation dependency in monthly mean minimum temperature in the Tibetan Plateau and its surroundings, and such a tendency may continue or even strengthen under future global warming conditions. However, some studies fails to find the relationship between warming amplitude and elevation in various mountainous regions around the world (Vuille and Bradley, 2000; Pepin and Seidel, 2005; Pepin and Lundquist, 2008; You et al., 2010a). When elevation was below 350 m, the situation was completely opposite. That is TN10P, FD, CSDI and DTR exhibited statistically significant positive correlations while TX90P, SU, TR, TNn, TNx and TXx showed significant negative correlations. This meant that the warming rates in temperature indices increased with decreasing altitude, which has never been discovered in YRB nor reported in other parts of the word. In general, the population density and the process of urbanization are greater in regions where stations with elevation lower than 350 m mainly located. As a result, this phenomenon may be mainly ascribed to the dense population distribution and rapid urbanization.

Table 5
Correlation coefficients between trends in temperature indices and elevation in the Yangtze River Basin during 1960–2012.

Index	Elevation >350 m	Elevation ≤350 m
TN10p	−0.49**	0.48**
TN90p	0.28*	−0.08
TX10P	−0.41**	0.22
TX90p	0.10	−0.29**
FD	−0.29**	0.56**
SU	0.18	−0.59**
ID	−0.32**	-
TR	-	−0.30**
TNn	0.39**	−0.37**
TNx	0.25*	−0.60**
TXn	0.12	−0.18
TXx	0.09	−0.20**
CSDI	−0.36**	0.47**
WSDI	0.20	−0.12
DTR	−0.34**	0.29**

* Values are significant at the 5% level.
** Values are significant at the 1% level.

6. Conclusions

Using a full set of the temperature indices recommended by ETCCDI, a better understanding of observed changes in temperature extremes is gained for the YRB during 1960–2012. Major results and conclusions are as follows. During 1960–2012, all the temperature indices revealed widespread significant changes associated with global warming over most parts of the YRB. The warming in minimum temperature indices, i.e.TN10P, TN90P, FD, TNn, TNx and CSDI, was of greater magnitudes than those of the maximum temperature indices such as TX10P, TX90P, ID, TXn, TXx and WSDI, consistent with many previous studies. Geographically, the most significant warming occurred in the eastern Tibet Plateau and northeastern YRB, indicating that the mountainous regions and populous regions are more sensitive and vulnerable to climate change. There are many factors contributing to the surface warming in the YRB, including the anthropogenic greenhouse gases, cloud cover, Asian brown clouds and land use changes as well as the atmospheric circulation change. However the exact impacts of these factors on extreme temperature events were not discussed in this study and further works are needed. But the analysis of elevation dependency of climatic warming showed that there are strong relationship between trend magnitudes and elevation for most temperature indices. The warming rates increased as elevation increases when elevation is above 350 m, but decreased as elevation increases when elevation is below 350 m. The latter may likely be attributed to the population increases, rapid industrialization and urbanization in the low lying region of the YRB. This conclusion needs to be further confirmed in future with longer records.

Differences in the variations of temperature indices are pronounced between the two periods of 1960–1985 and 1986–2012. During 1960–1985, the changes were much less spatially coherent compared with those during 1986–2012. Almost all temperature indices indicated a cooling trend for the YRB as a whole, but statistically significant changes were mainly detected in several indices. However, the eastern Tibet Plateau already demonstrated significant warming in indices like TN10P, FD, TNn, TXx and CSDI. For the period of 1986–2012, the warming was extraordinarily clear for the warm-related indices, more than doubling the changing rates of 1960–2012. Accordingly, we concluded that the warming in the YRB was mainly due to that in 1986–2012. This study also found a few trends that were inconsistent with previous studies. For example, DTR exhibited significant decreasing trends for most regions during 1960–2012. However, the decreasing trend all occurred in 1960–1985, while increasing trends were found in all subregions and the whole YRB during 1986–2012.

The Tibet Plateau is an important source of fresh water for the region, and has a great impact on the Asian monsoon systems (Liu et al., 2009). Warming in the Tibet Plateau has caused far-reaching eco-environmental problems such as glacier shrinkage (Su and Shi, 2002), permafrost melting (Chen and Wu, 2007) and vegetation change (Xu and Liu, 2007), and may threaten the available water resources for hundreds of millions of people residing in the middle and lower reaches of YRB. Therefore, proper governmental actions should be taken to cope with the changing weather and climate extremes in YRB.

Acknowledgements

This study is founded by the 948 Project of Ministry of Agriculture of China (Grant No. 2010-S16). We greatly appreciate the Grazinglands Research Laboratory, USDA-ARS for hosting the first author's visit and for supporting this research, and the National Climatic Centre (NCC) of the China Meteorological Administration (CMA) for providing the data.

References

Aguilar, E., Peterson, T.C., Obando, P.R., Frutos, R., Retana, J.A., Solera, M., Soley, J., García, I.G., Araujo, R.M., Santos, A.R., Valle, V.E., Brunet, M., Aguilar, L., Álvarez, L., Bautista, M., Castañón, C., Herrera, L., Ruano, E., Sinay, J.J., Sánchez, E., Oviedo, G.I.H., Obed, F., Salgado, J.E., Vázquez, J.L., Baca, M., Gutiérrez, M., Centella, C., Espinosa, J., Martínez, D., Olmedo, B., Ojeda Espinoza, C.E., Núñez, R., Haylock, M., Benavides, H., Mayorga, R., 2005. Changes in precipitation and temperature extremes in Central America and northern South America, 1961–2003. J. Geophys. Res. 110, D23107. http://dx.doi.org/10.1029/2005JD006119.

Alexander, L.V., Zhang, X., Peterson, T.C., Caesar, J., Gleason, B., Klein Tank, A.M.G., Haylock, M., Collins, D., Trewin, B., Rahimzadeh, F., Tagipour, A., Rupa Kumar, K., Revadekar, J., Griffiths, G., Vincent, L., Stephenson, D.B., Burn, J., Aguilar, E., Brunet, M., Taylor, M., New, M., Zhai, P., Rusticucci, M., Vazquez-Aguirre, J.L., 2006. Global observed changes in daily climate extremes of temperature and precipitation. J. Geophys. Res. 111, D05109. http://dx.doi.org/10.1029/2005JD006290.

Beniston, M., 2003. Climatic change in mountain regions: a review of possible impacts. Clim. Chang. 59 (1–2), 5–31.

Beniston, M., Rebetez, M., 1996. Regional behavior of minimum temperatures in Switzerland for the period 1979–1993. Theor. Appl. Climatol. 53, 231–243. http://dx.doi.org/10.1007/BF00871739.

Cannarozzo, M., Noto, L.V., Viola, F., 2006. Spatial distribution of rainfall trends in Sicily (1921–2000). Phys. Chem. Earth 31, 1201–1211. http://dx.doi.org/10.1016/j.pce.2006.03.022.

Chen, G.D., Wu, T.H., 2007. Responses of permafrost to climate change and their environmental significance, Qinghai-Tibet Plateau. J. Geophys. Res. 112, F02S03. http://dx.doi.org/10.1029/2006JF000631.

Chen, B.D., Chao, W.C., Liu, X.D., Lau, W.K.M., 2003. Enhanced climatic warming in the Tibetan Plateau due to doubling CO2: a model study. Clim. Dyn. 20 (4), 401–413.

Diaz, H.F., Bradley, R.S., 1997. Temperature variations during the last century at high elevation sites. Clim. Chang. 36 (3–4), 253–279.

Ding, Y.H., Chan, J.C.L., 2005. The East Asian summer monsoon: an overview. Meteorol. Atmos. Phys. 89 (1–4), 117–142.

Du, Y., Xie, Z.Q., Zeng, Y., Shi, Y.F., Wu, J.G., 2007. Impacts of urban expansion on regional temperature change in the Yangtze River Delta. J. Geogr. Sci. 17 (4), 387–398.

Duan, A.M., Wu, G.X., 2006. Change of cloud amount and the climate warming on the Tibetan Plateau. Geophys. Res. Lett. 33 (22), L22704. http://dx.doi.org/10.1029/2006GL027946.

Duan, A.M., Wu, G.X., Zhang, Q., Liu, Y.M., 2006. New proofs of the recent climate warming over the Tibetan Plateau as a result of the increasing greenhouse gases emissions. Chin. Sci. Bull. 51 (11), 1396–1400.

Easterling, D.R., Gerald, A.M., Camille, P., Stanley, A.C., Thomas, R.K., Linda, O.M., 2000a. Climate extremes: observations, modeling, and impacts. Science 289 (5487), 2068–2074.

Easterling, D.R., Evans, J.L., Groisman, P.Y., Karl, T.R., Kunkel, K.E., Ambenje, P., 2000b. Observed variability and trends in extreme climate events: a brief review. Bull. Am. Meteorol. Soc. 81 (3), 417–425. http://dx.doi.org/10.1175/1520-0477(2000)081<0417:OVATIE>2.3.CO;2.

Easterling, D.R., Alexander, L.V., Mokssit, A., Detemmerman, V., 2003. Cl/CLIVAR workshop to develop priority climate indices. Bull. Am. Meteorol. Soc. 84 (10), 1403–1407. http://dx.doi.org/10.1175/BAMS-84-10-1403.

Frauenfeld, O.W., Zhang, T.J., Serreze, M.C., 2005. Climate change and variability using European Centre for medium-range weather forecasts reanalysis (ERA-40) temperatures on the Tibetan Plateau. J. Geophys. Res. 110, D02101. http://dx.doi.org/10.1029/2004JD005230.

Fu, G.B., Yu, J.J., Yu, X.B., Ouyang, R.L., Zhang, Y.C., Wang, P., Liu, W.B., 2013. Temporal variation of extreme rainfall events in China, 1961–2009. J. Hydrol. 487, 48–59. http://dx.doi.org/10.1016/j.jhydrol.2013.02.021.

Fyfe, J.C., Flato, G.M., 1999. Enhanced climate change and its detection over the rocky mountains. J. Clim. 12 (1), 230–243. http://dx.doi.org/10.1175/1520-0442-12.1.230.

Gao, H., 2009. China's snow disaster in 2008, who is the principal player? Int. J. Climatol. 29 (14), 2191–2196.

Giorgi, F., Hurrel, J.W., Marinucci, M.R., Beniston, M., 1997. Elevation dependency of the surface climate change signal: a model study. J. Clim. 10 (2), 288–296. http://dx.doi.org/10.1175/1520-0442(1997)010<0288:EDOTSC>2.0.CO;2.

Harlan, S.L., Ruddell, D.M., 2011. Climate change and health in cities: impacts of heat and air pollution and potential co-benefits from mitigation and adaptation. Curr. Opin. Environ. Sustain. 3 (3), 126–134. http://dx.doi.org/10.1016/j.cosust.2011.01.001.

He, C., Shi, P., Li, J., Chen, J., Pan, Y., Li, J., Zhuo, L., Ichinose, T., 2006. Restoring urbanization process in China in the 1990s by using non-radiance-calibrated DMSP/OLS nighttime light imagery and statistical data. Chin. Sci. Bull. 51 (13), 1614–1620.

Hegerl, G.C., Zwiers, F.W., Stott, P.A., Kharin, V.V., 2004. Detectability of anthropogenic changes in annual temperature and precipitation extremes. J. Clim. 17 (19), 3683–3700. http://dx.doi.org/10.1175/1520-0442(2004)0172.0.CO;2.

Huynen, M.M., Martens, P., Schram, D., Weijenberg, M.P., Kunst, A.E., 2001. The impact of heat waves and cold spells on mortality rates in the Dutch population. Environ. Health Perspect. 109 (5), 463–470.

IPCC, 2007. Climate change 2007: the physical science basis. Contribution of Working Group I to the Fourth Assessment Report of the Intergovernmental Panel on Climate Change. Cambridge University Press, Cambridge, United Kingdom and New York, NY, USA.

IPCC, 2013. Climate change 2013: the physical science basis. Contribution of Working Group I to the Fifth Assessment Report of the Intergovernmental Panel on Climate Change. Cambridge University Press, Cambridge, United Kingdom and New York, NY, USA.

Jaagus, J., 2006. Climatic changes in Estonia during the second half of the 20th century in relationship with changes in large-scale atmospheric circulation. Theor. Appl. Climatol. 83, 77–88.

Jiang, T., Su, B.D., Hartmann, H., 2007. Temporal and spatial trends of precipitation and river flow in the Yangtze River Basin, 1961–2000. Geomorphology 85 (3–4), 143–154. http://dx.doi.org/10.1016/j.geomorph.2006.03.015.

Kampata, J.M., Parida, B.P., Moalafhi, D.B., 2008. Trend analysis of rainfall in the headstreams of the Zambezi River Basin in Zambia. Phys. Chem. Earth 33 (8–13), 621–625. http://dx.doi.org/10.1016/j.pce.2008.06.012.

Kang, S.C., Xu, Y.W., You, Q.L., Flügel, W., Pepin, N., Yao, T.D., 2010. Review of climate and cryospheric change in the Tibetan Plateau. Environ. Res. Lett. 5, 015101. http://dx.doi.org/10.1088/1748-9326/5/1/015101.

Karl, T.R., Nicholls, N., Ghazi, A., 1999. CLIVAR/GCOS/WMO workshop on indices and indicators for climate extremes: Workshop summary. Clim. Chang. 42 (1), 3–7.

Katz, R.W., Brown, B.G., 1992. Extreme events in a changing climate: variability is more important than averages. Clim. Chang. 21 (3), 289–302.

Kendall, M.G., 1962. Rank correlation methods. 3rd ed. Hafner Publishing Company, New York.

Klein Tank, A.M.G., Können, G.P., 2003. Trends in indices of daily temperature and precipitation extremes in Europe, 1946–99. J. Clim. 16 (22), 3665–3680. http://dx.doi.org/10.1175/1520-0442(2003)016<3665:TIIODT>2.0.CO;2.

Klein Tank, A.M.G., Peterson, T.C., Quadir, D.A., Dorji, S., Zou, X., Tang, H., Santhosh, K., Joshi, U.R., Jaswai, A.K., Kolli, R.K., Sikder, A.B., Deshpande, N.R., Revadekar, J.V., Yeleuova, K., Vandasheva, S., Faleyeva, M., Gomboluudev, P., Budhathoki, K.P., Hussain, A., Afzaal, M., Chandrapala, L., Anvar, H., Amanmurad, D., Asanova, V.S., Jones, P.D., New, M.G., Spektorman, T., 2006. Changes in daily temperature and precipitation extremes in central and south Asia. J. Geophys. Res. 111, D16105. http://dx.doi.org/10.1029/2005JD006316.

Kunkel, K.E., Roger, A.P., Stanley, A.C., 1999. Temporal fluctuations in weather and climate extremes that cause economic and human health impacts: a review. Bull. Am. Meteorol. Soc. 80, 1077–1098. http://dx.doi.org/10.1175/1520-0477(1999)080<1077:TFIWAC>2.0.CO;2.

Labat, D., Goddéris, Y., Probst, J.L., Guyot, J.L., 2004. Evidence for global runoff increase related to climate warming. Adv. Water Resour. 27 (6), 631–642. http://dx.doi.org/10.1016/j.advwatres.2004.02.020.

Li, X., Zhou, X., Li, W., 1995. The cooling of Sichuan Province in recent 40 years and its probable mechanisms. Acta Meteorol. Sin. 9, 57–68 (in chinese).

Li, Z., Zheng, F.L., Liu, W.Z., Flanagan, D.C., 2010. Spatial distribution and temporal trends of extreme temperature and precipitation events on the Loess Plateau of China during 1961–2007. Quat. Int. 226 (1–2), 92–100. http://dx.doi.org/10.1016/j.quaint.2010.03.003.

Li, Q.F., Yu, M.X., Lu, G.B., Cai, T., Bai, X., Xia, Z.Q., 2011a. Impacts of the Gezhouba and Three Gorges reservoirs on the sediment regime in the Yangtze River, China. J. Hydrol. 403 (3–4), 224–233. http://dx.doi.org/10.1016/j.jhydrol.2011.03.043.

Li, Z.X., He, Y.Q., Wang, C.F., Wang, X.F., Xin, H.J., Zhang, W., Cao, W.H., 2011b. Spatial and temporal trends of temperature and precipitation during 1960–2008 at the Hengduan Mountains, China. Quat. Int. 236 (1–2), 127–142. http://dx.doi.org/10.1016/j.quaint.2010.05.017.

Li, J., Dong, W.J., Yang, Z.W., 2012a. Changes of climate extremes of temperature and precipitation in summer in eastern China associated with changes in atmospheric circulation in East Asia during 1960–2008. Chin. Sci. Bull. 57 (15), 1856–1861.

Li, Z.X., He, Y.Q., Wang, P.Y., Theakstone, W.H., An, W.L., Wang, X.F., Lu, A.G., Zhang, W., Cao, W.H., 2012b. Changes of daily climate extremes in southwestern China during 1961–2008. Global Planet. Chang. 80–81, 255–272. http://dx.doi.org/10.1016/j.gloplacha.2011.06.008.

Liang, E.Y., Shao, X.M., Qin, N.S., 2008. Tree-ring based summer temperature reconstruction for the source region of the Yangtze River on the Tibetan Plateau. Global Planet. Chang. 61 (3–4), 313–320. http://dx.doi.org/10.1016/j.gloplacha.2007.10.008.

Liang, K., Bai, P., Li, J.J., Liu, C.M., 2014. Variability of temperature extremes in the Yellow River basin during 1961–2011. Quat. Int. 336, 52–64. http://dx.doi.org/10.1016/j.quaint.2014.02.007.

Liu, X.D., Chen, B.D., 2000. Climatic warming in the Tibetan Plateau during recent decades. Int. J. Climatol. 20 (14), 1729–1942.

Liu, X., Cheng, Z.G., Yan, L.B., Yin, Z.Y., 2009. Elevation dependency of recent and future minimum surface air temperature trends in the Tibetan Plateau and its surroundings. Global Planet. Chang. 68 (3), 164–174. http://dx.doi.org/10.1016/j.gloplacha.2009.03.017.

Loáiciga, H.A., Valdes, J.B., Vogel, R., Garvey, J., Schwarz, H., 1996. Global warming and the hydrological cycle. J. Hydrol. 174 (1–2), 83–127. http://dx.doi.org/10.1016/0022-1694(95)02753-X.

Luber, G., McGeehin, M., 2008. Climate change and extreme heat events. Am. J. Prev. Med. 35 (5), 429–435. http://dx.doi.org/10.1016/j.amepre.2008.08.021.

Ma, W.J., Xu, X.H., Peng, L., Kan, H.D., 2011. Impact of extreme temperature on hospital admission in Shanghai, China. Sci. Total Environ. 409 (19), 3634–3637. http://dx.doi.org/10.1016/j.scitotenv.2011.06.042.

Mann, H.B., 1945. Non–parametric tests again trend. Econometrica 13, 245–259.

Meehl, G.A., Karl, T., Easterling, D.R., Changnon, S., Jr Pielke, R., Changnon, D., Evans, J., Groisman, P.Y., Knutson, T.R., Kunkel, K.E., Mearns, L.O., Parmesan, C., Pulwarty, R., Root, T., Sylves, R.T., Whetton, P., Zwiers, F., 2000. An introduction to trends in extreme weather and climate events: observations, socioeconomic impacts, terrestrial ecological impacts, and model projections. Bull. Am. Meteorol. Soc. 81 (3), 413–416. http://dx.doi.org/10.1175/1520-0477(2000)081<0413:AITTIE>2.3.CO;2.

Moberg, A., Jones, P.D., Lister, D., Walther, A., Brunet, M., Jacobeit, J., Alexander, L.V., Della-Marta, P.M., Luterbacher, J., Yiou, P., Chen, D.L., Klein Tank, A.M.G., Saladié, O., Sigró, J., Aguilar, E., Alexandersson, H., Almarza, C., Auer, I., Barriendos, M., Begert, M., Bergström, H., Böhm, R., Butler, C.J., Caesar, J., Drebs, A., Founda, D., Gerstengarbe, F.W., Micela, G., Maugeri, M., Österle, H., Pandzic, K., Petrakis, M., Srnec, L., Tolasz, R., Tuomenvirta, H., Werner, P.C., Linderholm, H., Philipp, A., Wanner, H., Xoplaki, E., 2006. Indices for daily temperature and precipitation extremes in Europe analyzed for the period 1901–2000. J. Geophys. Res. 111, D22106. http://dx.doi.org/10.1029/2006JD007103.

New, M., Hewitson, B., Stephenson, D.B., Tsiga, A., Kruger, A., Manhique, A., Gomez, B., Coelho, C.A.S., Masisi, D.N., Kululanga, E., Mbambalala, E., Adesina, F., Saleh, H., Kanyanga, J., Adosi, J., Bulane, L., Fortunata, L., Mdoka, M.L., Lajoie, R., 2006. Evidence of trends in daily climate extremes over Southern and West Africa. J. Geophys. Res. 111, D14102. http://dx.doi.org/10.1029/2005JD006289.

O'Neal, M.R., Nearing, M.A., Vining, R.C., Southworth, J., Pfeifer, R.A., 2005. Climate change impacts on soil erosion in Midwest United States with changes in crop management. Catena 61 (2–3), 165–184. http://dx.doi.org/10.1016/j.atena.2005.03.003.

Pepin, N.C., Lundquist, J.D., 2008. Temperature trends at high elevations: patterns across the globe. Geophys. Res. Lett. 35, L14701. http://dx.doi.org/10.1029/2008GL034026.

Pepin, N.C., Seidel, D.J., 2005. A global comparison of surface and free-air temperatures at high elevations. J. Geophys. Res. 110, D03104. http://dx.doi.org/10.1029/2004JD005047.

Peterson, T.C., Taylor, M.A., Demeritte, R., Duncombe, D.L., Burton, S., Thompson, F., Porter, A., Mercedes, M., Villegas, E., Semexant Fils, R., Klein Tank, A.M.K., Martis, A., Warner, R., Joyette, A., Mills, W., Alexander, L.V., Gleason, B., 2002. Recent changes in climate extremes in the Caribbean region. J. Geophys. Res. 107, 4601. http://dx.doi.org/10.1029/2002JD002251.

Rahimzadeh, F., Asgari, A., Fattahi, E., 2009. Variability of extreme temperature and precipitation in Iran during recent decades. Int. J. Climatol. 29 (3), 329–343.

Ramanathan, V., Ramana, M.V., Roberts, G., Kim, D., Corrigan, C., Chung, C., Winker, D., 2007. Warming trends in Asia amplified by brown cloud solar absorption. Nature 448 (7153), 575–578.

Rohde, R., Muller, R.A., Jacobsen, R., Muller, E., Perlmutter, S., Rosenfeld, A., Wurtele, J., Groom, D., Wickham, C., 2013. A new estimate of the average earth surface land temperature spanning 1753 to 2011. Geoinfor. Geostat. 1 (1). http://dx.doi.org/10.4172/2327-4581.1000101 (An Overview).

Sang, Y.F., 2012. Spatial and temporal variability of daily temperature in the Yangtze River Delta, China. Atmos. Res. 112, 12–24. http://dx.doi.org/10.1016/j.atmosres.2012.04.006.

Sang, Y.F., Wang, Z.G., Liu, C.M., 2012. Spatial and temporal variability of daily temperature during 1961–2010 in the Yangtze River Basin, China. Quat. Int. 304, 33–42. http://dx.doi.org/10.1016/j.quaint.2012.05.026.

Sen, P.K., 1968. Estimates of the regression coefficient based on Kendall's tau. J. Am. Stat. Assoc. 63, 1379–1389.

Skansi, M.M., Brunet, M., Sigró, J., Aguilar, E., Groening, J.A.A., Bentancur, O.J., Geier, Y.R.C., Amaya, R.L.C., Jácome, H., Ramos, A.M., Rojas, C.O., Pasten, A.M., Mitro, S.S., Jiménez, C.V., Martínez, R., Alexander, L.V., Jones, P.D., 2013. Warming and wetting signals emerging from analysis of changes in climate extreme indices over South America. Global Planet. Chang. 100, 295–307. http://dx.doi.org/10.1016/j.gloplacha.2012.11.004.

Some'e, S.B., Ezani, A., Tabari, H., 2012. Spatiotemporal trends and change point of precipitation in Iran. Atmos. Res. 113, 1–12. http://dx.doi.org/10.1016/j.atmosres.2012.04.016.

Su, Z., Shi, Y., 2002. Response of monsoonal temperate glaciers to global warming since the Little Ice Age. Quat. Int. 97–98, 123–131. http://dx.doi.org/10.1016/S1040-6182(02)00057-5.

Su, B.D., Jiang, T., Jin, W.B., 2006. Recent trends in observed temperature and precipitation extremes in the Yangtze River basin, China. Theor. Appl. Climatol. 83, 139–151. http://dx.doi.org/10.1007/s00704-005-0139-y.

Su, B.D., Gemmer, M., Jiang, T., 2008. Spatial and temporal variation of extreme precipitation over the Yangtze River Basin. Quat. Int. 186 (1), 22–31. http://dx.doi.org/10.1016/j.quaint.2007.09.001.

Tabari, H., Talaee, P.H., 2011. Temporal variability of precipitation over Iran: 1966–2005. J. Hydrol. 396 (3–4), 313–320. http://dx.doi.org/10.1016/j.jhydrol.2010.11.034.

Tabari, H., Nikbakht, J., Some'e, B.S., 2011. Investigation of groundwater level fluctuations in the north of Iran. Environ. Earth Sci. 66, 231–243. http://dx.doi.org/10.1007/s12665-011-1229-z.

Tan, J.G., Zheng, Y.F., Song, G.X., Kalkstein, L.S., Kalkstein, A.J., Tang, X., 2007. Heat wave impacts on mortality in Shanghai, 1998 and 2003. Int. J. Biometeorol. 51 (3), 193–200. http://dx.doi.org/10.1007/s00484-006-0058-3.

The China Meteorological Administration. China's top ten weather climate events in 2013. Available at, http://www.weather.com.cn/news/2013/11/2011013_3.shtml (2013/11/28).

Trenberth, K.E., Jones, P.D., Ambenje, P., Bojariu, R., Easterling, D., Klein Tank, A.M.K., Parker, D., Rahimzadeh, F., Renwick, J.A., Rusticucci, M., Soden, B., Zhai, P., 2007. Observations: surface and atmospheric climate change. In: Solomon, S., Qin, D., Manning, M., Chen, Z., Marquis, M., Averyt, K.B., Tignor, M., Miller, H.L. (Eds.), Climate change 2007: the physical science basis. Contribution of Working Group I to the Fourth Assessment Report of the Intergovernmental Panel on Climate Change. Cambridge University Press, Cambridge, United Kingdom and New York, NY, USA, p. 336.

Vincent, L.A., Mekis, E., 2006. Changes in daily and extreme temperature and precipitation indices for Canada over the twentieth century. Atmos. Ocean 44, 177–193. http://dx.doi.org/10.1029/2005JD006316.

Vincent, L.A., Peterson, T.C., Barros, V.R., Marino, M.B., Rusticucci, M., Carrasco, G., Ramirez, E., Alves, L.M., Ambrizzi, T., Berlato, M.A., Grimm, A.M., Marengo, J.A., Molion, L., Moncunill, D.F., Rebello, E., Anunciacao, Y.M.T., Quintana, J., Santos, J.L., Baez, J., Coronel, G., Garcia, J., Trebejo, I., Bidegain, M., Haylock, M.R., Karoly, D., 2005. Observed trends in indices of daily temperature extremes in South America 1960–2000. J. Clim. 18 (23), 5011–5023. http://dx.doi.org/10.1175/JCLI3589.1.

Vose, R.S., Easterling, D.R., Gleason, B., 2005. Maximum and minimum temperature trends for the globe: An update through 2004. Geophys. Res. Lett. 32, L23822. http://dx.doi.org/10.1029/2005GL024379.

Vuille, M., Bradley, R.S., 2000. Mean annual temperature trends and their vertical structure in the topical Andes. Geophys. Res. Lett. 27, 3885–3888.

Wang, B.L., Zhang, M.J., Wei, J.L., Wang, S.J., Li, S.S., Ma, Q., Li, X.F., Pan, S.K., 2013a. Changes in extreme events of temperature and precipitation over Xinjiang, northwest China, during 1960–2009. Quat. Int. 298, 141–151. http://dx.doi.org/10.1016/j.quaint.2012.09.010.

Wang, S.J., Jiao, S.T., Xin, H.J., 2013b. Spatio-temporal characteristics of temperature and precipitation in Sichuan Province, Southwestern China, 1960–2009. Quat. Int. 286, 103–115. http://dx.doi.org/10.1016/j.quaint.2012.04.030.

Wang, S.J., Zhang, M.J., Wang, B.L., Sun, M.P., Li, X.F., 2013c. Recent changes in daily extremes of temperature and precipitation over the western Tibetan Plateau, 1973–2011. Quat. Int. http://dx.doi.org/10.1016/j.quaint.2013.03.037.

Wang, Q., Zhang, M.J., Wang, S.J., Ma, Q., Sun, M.P., 2014. Changes in temperature extremes in the Yangtze River Basin, 1962–2011. J. Geogr. Sci. 24, 59–75. http://dx.doi.org/10.1007/s11442-014-1073-7.

Wild, M., Ohmura, A., Makowski, K., 2007. Impact of global dimming and brightening on global warming. Geophys. Res. Lett. 34, L04702. http://dx.doi.org/10.1029/2006GL028031.

Xie, Z.Q., Du, Y., Zeng, Y., Yan, M.L., Zhu, C.Y., 2010. Accelerated human activities affecting the spatial pattern of temperature in the Yangtze River Delta. Quat. Int. 226 (1–2), 112–121. http://dx.doi.org/10.1016/j.quaint.2010.04.027.

Xu, W., Liu, X., 2007. Response of vegetation in the Qinghai-Tibet Plateau to global warming. Chin. Geogr. Sci. 17, 151–159.

Xu, M., Chang, C.P., Fu, C.B., Qi, Y., Robock, A., Robinson, D., Zhang, H.M., 2006. Steady decline of east Asian monsoon winds, 1969–2000: Evidence from direct ground measurements of wind speed. J. Geophys. Res. 111, D24111. http://dx.doi.org/10.1029/2006JD007337.

Xu, Y., Xu, C.H., Gao, X.J., Luo, Y., 2009. Projected changes in temperature and precipitation extremes over the Yangtze River Basin of China in the 21st century. Quat. Int. 208 (1–2), 44–52. http://dx.doi.org/10.1016/j.quaint.2008.12.020.

Yang, X., Zhang, Y., Zhang, W., Yan, Y., Wang, Z., Ding, M., Chu, D., 2006. Climate change in Mt. Qomolangma region since 1971. J. Geogr. Sci. 16, 326–336.

You, Q.L., Kang, S.C., Aguilar, E., Yan, Y., 2008. Changes in daily climate extremes in the eastern and central Tibetan Plateau during 1961–2005. J. Geophys. Res. 113, D07101. http://dx.doi.org/10.1029/2007JD009389.

You, Q.L., Kang, S.C., Pepin, N., Flügel, W., Yan, Y.P., 2010a. Relationship between temperature trend magnitude, elevation and mean temperature in the Tibetan Plateau from homogenized surface stations and reanalysis data. Global Planet. Chang. 71 (1–2), 124–133. http://dx.doi.org/10.1016/j.gloplacha.2010.01.020.

You, Q.L., Kang, S.C., Pepin, N., Flügel, W., Lorenzo, A.S., Yan, Y.P., Zhang, Y.J., 2010b. Climate warming and associated changes in atmospheric circulation in the eastern and central Tibetan Plateau from a homogenized dataset. Global Planet. Chang. 72 (1–2), 11–24. http://dx.doi.org/10.1016/j.gloplacha.2010.04.003.

You, Q., Kang, S.C., Aguilar, E., Pepin, N., Flügel, W., Yan, Y.P., Xu, Y.W., Zhang, Y.J., Huang, J., 2011. Changes in daily climate extremes in China and their connection to the large scale atmospheric circulation during 1961–2003. Clim. Dyn. 36 (11–12), 2399–2417. http://dx.doi.org/10.1007/s00382-009-0735-0.

Yu, F.L., Chen, Z.Y., Ren, X.Y., Yang, G.F., 2009. Analysis of historical floods on the Yangtze River, China: Characteristics and explanations. Geomorphology 113, 210–216.

Zhai, P.M., Pan, X.H., 2003. Trends in temperature extremes during1951–1999 in China. Geophys. Res. Lett. 30 (17), 1913. http://dx.doi.org/10.1029/2003GL018004.

Zhai, P.M., Zhang, X.B., Wan, H., Pan, X.H., 2005. Trends in total precipitation and frequency of daily precipitation extremes over China. J. Clim. 18 (7), 1096–1108. http://dx.doi.org/10.1175/JCLI-3318.1.

Zhang, T., 2007. Perspectives on environmental study of response to climatic and land cover/land use change over the Qinghai-Tibetan plateau: an introduction. Arct. Antarct. Alp. Res. 39, 631–634. http://dx.doi.org/10.1657/1523-0430(07-513)[ZHANG]2.0.CO;2.

Zhang, X.B., Vincent, L.A., Hogg, W.D., Niitsoo, A., 2000. Temperature and precipitation trends in Canada during the 20th century. Atmos. Ocean 38 (3), 395–429.

Zhang, Q., Jiang, T., Gemmer, M., Becker, S., 2005a. Precipitation, temperature and runoff analysis from 1950 to 2002 in the Yangtze basin, China. Hydrol. Sci. J. 50, 65–80.

Zhang, X.B., Aguilar, E., Sensoy, S., Melkonyan, H., Tagiyeva, U., Ahmed, N., Kutaladze, N., Rahimzadeh, F., Taghipour, A., Hantosh, T.H., Albert, P., Semawi, M., Karam Ali, M., Said Al-Shabibi, M.H., Al-Oulan, Z., Zatari, T., Al Dean Khelet, I., Hamoud, S., Sagir, R., Demircan, M., Eken, M., Adiguzel, M., Alexander, L.V., Peterson, T.C., Wallis, T., 2005b. Trends in Middle East climate extreme indices from 1950 to 2003. J. Geophys. Res. 110, D22104. http://dx.doi.org/10.1029/2005JD006181.

Zhang, Q., Xu, C.Y., Jiang, T., Wu, Y.J., 2007. Possible influence of ENSO on annual maximum streamflow of the Yangtze River, China. J. Hydrol. 333 (2–4), 265–274. http://dx.doi.org/10.1016/j.jhydrol.2006.08.010.

Zhang, Q., Xu, C.Y., Zhang, Z.X., David Chen, Y.Q., Liu, C.L., Lin, H., 2008. Spatial and temporal variability of precipitation maxima during 1960–2005 in the Yangtze River basin and possible association with large-scale circulation. J. Hydrol. 353 (3–4), 215–227. http://dx.doi.org/10.1016/j.jhydrol.2007.11.023.

Zhang, G.L., Dong, J.W., Zhou, C.P., Xu, X.L., Wang, M., Ouyang, H., Xiao, X.M., 2013. Increasing cropping intensity in response to climate warming in Tibetan Plateau, China. Field Crop Res. 142, 36–46. http://dx.doi.org/10.1016/j.fcr.2012.11.021.

Zhao, G.J., Hörmann, G., Fohrer, N., Gao, J.F., Zhai, J.Q., Zhang, Z.X., 2009. Spatial and temporal characteristics of wet spells in the Yangtze River Basin from 1961 to 2003. Theor. Appl. Climatol. 98 (1), 107–117. http://dx.doi.org/10.1007/s00704-008-0099-0.

Zhao, G.J., Mu, X.M., Hörmann, G., Fohrer, N., Xiong, M., Su, B.D., Li, X.C., 2012. Spatial patterns and temporal variability of dryness/wetness in the Yangtze River Basin, China. Quat. Int. 282, 5–13. http://dx.doi.org/10.1016/j.quaint.2011.10.020.